

Master Thesis



Escola Tècnica Superior
d'Enginyeria Industrial de Barcelona

**Analysis of a Total Integration of Renewable Energy
Through a Dynamic Virtual Power Plant Model and
the Use of Hydrogen as a Method of Energy
Production Stabilization**

Author:

Danilo Silva Lévano

Director:

Oriol Gomis Bellmunt, PhD



Barcelona, July 2nd 2023

Acknowledgment

To my family, thank you for being my refuge, my strength and my inspiration. Your loving presence has been the foundation upon which I have built my dreams. Your dedication and sacrifice have been invaluable, and I will always be grateful for all that you have done for me.

To my professors at UPC, in particular Orio Gomis, I would like to express my sincere appreciation for your passion for teaching and your dedication to our academic achievements. Your guidance and knowledge have been a constant source of inspiration and motivation. Thank you for challenging me to push my limits and for believing in my potential.

To all of you, family and professors, I want to thank you for being my support network and for giving me the confidence to pursue my goals. Your presence in my life has been a priceless gift, and I cannot express in words how much it means to me.

Once again, thank you from the bottom of my heart for being there for me. Your influence and love have made a significant difference in my life, and I will always be grateful for it.

Abstract

The growing need for change in the energy vector, the increasing popularity of renewable energies, as well as the European regulations to achieve zero emissions by 2050 (currently at 21.8% in Europe with a projection of 42.5% by 2030), prompt the analysis of scenarios for meeting the annual demand in three autonomous communities (Andalusia and Valencia) while considering the current electric grid and a new scenario with the most optimal distribution. This analysis involves simplifying the grid and utilizing a distributed virtual power plant (DVPP).

These scenarios consider increasing the share of renewables up to 99% and implementing hydrogen-based storage technologies to evaluate their economic impact on the levelized cost of energy and how it increases as the share of renewables grows. Prices for each available technology have been obtained to achieve a more realistic approximation. Variables such as capital expenditures (CAPEX), operating expenses (OPEX), fuel costs where applicable, and replacement costs have been considered, as the project analyses the system with a 50-year outlook, and some technologies have a lifespan shorter than this period.

The obtained results will be used to analyse the capacities of hydrogen plants in terms of power and storage, as well as their behaviour in balancing the grid as a supporting technology for intermittent generation sources such as wind and photovoltaic, and for managing potential energy surpluses.

Contents

1	Introduction.....	8
2	Background and definitions	10
2.1	Renewable energy sources	10
2.1.1	Biomass and biofuel energy	10
2.1.2	Geothermal energy	12
2.1.3	Hydropower.....	14
2.1.4	Photovoltaic energy	15
2.1.5	Solar thermal energy	27
2.1.6	Tidal and wave power.....	40
2.1.7	Wind power	45
2.2	Non-Renewable energy sources.....	51
2.2.1	Conventional power plants	51
2.2.2	Nuclear power.....	54
2.3	Energetic vector: Hydrogen	58
2.3.1	Production	58
2.3.2	Storage.....	59
2.3.3	Use	60
2.3.4	Scalability.....	61
2.4	Environmental European policies	63
3	Dynamic Virtual Power Plant (DVPP)	65
3.1	Definition	65
3.2	Ancillary services: Frequency and voltage	66
4	Geographic delimitation	70
4.1	Demand.....	71
4.2	Installed capacity	73
5	Methodology.....	74

5.1	Optimization method: Levelized Cost of Energy	74
5.2	System modelling	76
5.2.1	Elements included and constraints included in the model.....	76
5.2.2	General considerations	85
5.3	Optimization problem	86
5.3.1	Case 1 (Base case, limitation in installed capacity).....	86
5.3.2	Case 2 (increasing renewable share from 35 to 99%).....	88
5.3.3	Case 3 (increasing renewable share from 35 to 99% + Offshore)	91
5.3.4	Case 4 (Renewable share from 35 to 99% + Offshore + Hydro + H2) ...	94
6	Conclusions and future improvements	97
7	References	99

List of Figures

Illustration 1. Biomass to bioenergy conversion platforms [4].	11
Illustration 2. Layers of the Earth. Eboch, M. M. (2019). Geothermal Energy. United Kingdom: Raintree Publishers.	13
Illustration 3. Two main facilities for hydropower installations. Office of Energy Efficiency and Renewable Energy.	15
Illustration 4. Technologies and cell efficiencies developed. This plot is courtesy of the National Renewable Energy Laboratory, Golden, CO. 2023.	16
Illustration 5. p-n junction and carriers' concentrations.	18
Illustration 6. Visual description of the different quantum bands.	19
Illustration 7. Simplified band diagram considering ETL and HTL.	20
Illustration 8. Fill factor for a single solar cell.	22
Illustration 9. Current and power density vs cell voltage for an ideal solar cell.	22
Illustration 10. Ideal solar cell equivalent circuit model.	23
Illustration 11. Real solar cell equivalent circuit model.	24
Illustration 12. Standard solar spectrum at different conditions. Data is courtesy of the National Renewable Energy Laboratory, Golden, CO.	28
Illustration 13. Main components for a flat plate collector [10].	31
Illustration 14. Mainly flow direction in a flat plate collector with a storage tank [10].	33
Illustration 15. Typical efficiency curve for a flat plate collector.	35
Illustration 16. View of parabolic trough collector [10].	37
Illustration 17. Simplified scheme of a central solar receiver [10].	38
Illustration 18. Scheme of a Linear Fresnel [10].	38
Illustration 19. View of a parabolic dish [10].	39
Illustration 20. Rance Tidal Power Station [13].	41
Illustration 21. Tidal power plant cross section view and water flow directions [14].	42
Illustration 22. Representation of a point absorber buoy [15].	44
Illustration 23. Attenuator's main components [16].	44
Illustration 24. Scheme of an oscillating water column device (left) and Mutriku Wave Power plant (right) [16].	45
Illustration 25. Cross section of an overtopping device [17].	45

Illustration 26. A Darrieus wind turbine model VP100 (left), main components (right) [18].	46
Illustration 27. Overall components of a horizontal wind turbine [19].	47
Illustration 28. One-dimensional projected conditions [20].	49
Illustration 29. Typical turbine power curve for a Gamesa G80 model [21].	50
Illustration 30. Scheme for a diesel engine power plant [22].	51
Illustration 31. Scheme simplified of a conventional power plant [23].	52
Illustration 32. Scheme simplified of a cogeneration power plant [24].	53
Illustration 33. Fission reaction process.	56
Illustration 34. Typical-day demand profile per hour. Data is courtesy of REE.	72
Illustration 35. Base case Matching Generation / demand in Andalusia	87
Illustration 36. Base case Matching Generation / demand in Valencia	88
Illustration 37. Case 2 installed capacity vs Renewable share in Andalusia	89
Illustration 38. Case 2 installed capacity vs Renewable share in Valencia	89
Illustration 39. Case 2 LCOE vs Renewable share in Andalusia	90
Illustration 40. Case 2 LCOE vs Renewable share in Valencia	90
Illustration 41. Case 3 Installed Capacity vs Renewable share in Andalusia	92
Illustration 42. Case 3 Installed Capacity vs Renewable share in Valencia	92
Illustration 43. Case 2 LCOE vs Renewable share in Andalusia	93
Illustration 44. Case 2 LCOE vs Renewable share in Valencia	93
Illustration 45. Case 4 Installed Capacity vs Renewable share in Andalusia	95
Illustration 45. Case 4 Installed Capacity vs Renewable share in Valencia	95
Illustration 47. Case 4 LCOE vs Renewable share in Andalusia	96
Illustration 48. Case 4 LCOE vs Renewable share in Valencia	96

List of Tables

Table 1. Thickness and average temperatures for different Earth's layers. Own adaptation from [6].	13
Table 2. Highest efficiencies by cell technology. Own adaption from [8].	18
Table 3. Comparison of main concentrated solar plant technologies [11].	39
Table 4. Location of the selected places for new power plants in Andalusia.	71
Table 5. Installed capacity in Valencia for 2022. Data courtesy by REE.	73
Table 6. Installed capacity in Andalusia for 2022. Data courtesy by REE.	73

1 Introduction

Within the following pages, an electrical network will be analysed from the point of view of its integration with renewable sources in two regions. The main goal is to analyse how the integration of renewable sources affect the composition of the network. Factors as demand, renewable's penetration (% of renewable used to model the network), storage, cost variation and location of the renewable sources could affect the composition and LCOE of the Network.

The selected regions are Andalusia and Valencia. Some restrictions have been taken into account such as the possibility of installing renewables not only considering the availability of the resource but the suitability of the land.

For the generation scenarios, renewable sources such as Photovoltaic, Wind and Hydro and H2 storage and use to balance network are used in the analysis.

The analysis performed is a purely economic to provide information on the impact of the renewables and its penetration into the grid (new and existent one). An evaluation of LCOE obtained according to penetration of the renewables could help to decide for a percentage of penetration that represents the lower cost and the least curtailment of the generation.

The tools selected for the analysis is Pyomo which is Python based optimization module and Gurobi for the solver. Gurobi optimizer is a state-of-the-art solver for mathematical programming that takes advantage of a multi-core processors to solve the objective function.

For the analysis of raw data and graphic generation/evaluation, Microsoft Excel has been selected.

This project has been carried out in collaboration with Abraham Turcios Marquez, whose project "*Analysis of a Total Integration of Renewable Energy in Catalonia Through a Dynamic Virtual Power Plant Model and the Use of Hydrogen as a Method of Energy Production Stabilization*" application is specific to the region of Catalonia. The main differences with the development of this project are the application scenarios and the power limitations with respect to the current installed capacity. The

collaboration with Mr. Turcios Márquez has allowed a faster and more optimal implementation of the solutions as well as the analysis of both project results.

2 Background and definitions

2.1 Renewable energy sources

2.1.1 Biomass and biofuel energy

Biomass

A biomass source refers to organic matter that can be treated to extract hidden energy for useful work. There are various methods to convert this latent energy into the energy required for our needs.

It is important to note that biomass energy has been used since ancient times and played a significant role until the early 19th century, particularly in industrialized countries [1]. Commonly utilized materials included wood, charcoal, and agricultural residues.

In recent times, around 25 EJ (exajoules) of biomass energy were estimated to be utilized for cooking and heating in 2021 [2]. This consumption is predominantly seen in developing economies in Africa and Asia, where access to clean cooking is challenging, especially in rural areas.

It is crucial to distinguish biomass from hydrocarbon sources¹. Biomass is derived from renewable sources that can be sustainably managed, such as forests, crops, agricultural surplus, municipal organic waste, etc. On the other hand, hydrocarbon sources originate from non-renewable oil reservoirs and do not possess a significant renewable basis to meet human needs.

The biomass undergoes several stages from its natural state. Modern manufacturing processes involve specific conditions to prepare the matter according to technical requirements, enhancing energy efficiency conversion. The main steps involved are as follows:

- **Primary bioenergy:** This term describes biomass in its natural state before any conversion or processing takes place.

¹ Like biofuels, that will be developed in detail in the next paragraphs.

- **Final bioenergy:** This concept pertains to the biomass's end state, where it is transformed into solid, liquid, or gaseous fuels, ready to be directly used for a specific application.
- **Useful bioenergy:** This refers to the net energy obtained from the biomass source, taking into account the energy losses during conversion processes. It includes energy forms such as electricity and heat that can be effectively utilized.

Biofuels

The terminology used for biofuels encompasses various biobased products, including solids, liquids, and gases, derived from natural materials. In the modern context, examples of biofuels include bio-oil, bioethanol, biodiesel, and biogas (these can be obtained from microalgae) [3].

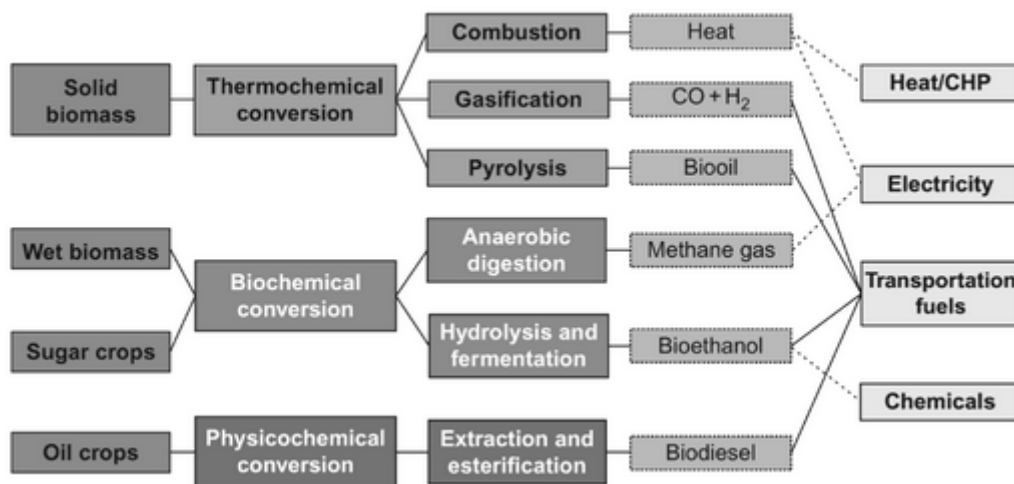


Illustration 1. Biomass to bioenergy conversion platforms [4].

Illustration 1 is referred about the usable energy obtained from different states: solid, gas, and liquid. Each state undergoes specific production processes that correspond to distinct types of conversion, as outlined below:

- **Thermochemical conversion:** This term pertains to the decomposition of organic matter through partial or complete oxidation, with thermal energy playing a crucial role in influencing the resulting products [5].
- **Physicochemical conversion:** This concept involves the breakdown of the physical organic structure, and one widely employed method for biomass decomposition is steam explosion pre-treatment [4].

- **Biochemical conversion:** This refers to the decomposition of organic matter through biological organisms that break down complex organic structures. One commonly used method for this type of conversion is anaerobic digestion.

It's worth noting that for solid fuels, raw biological matter can be utilized, which includes traditional biomass uses. Additionally, other examples of solid fuels include straw bales, briquettes, wood chips, and wood pallets.

2.1.2 Geothermal energy

Geothermal energy is a form of energy that originates from the thermal energy present beneath the Earth's crust. This energy is a result of the planet's formation and the decay of radioactive materials such as potassium, thorium, and uranium. Under specific geological conditions, the thermal energy can be harnessed to generate electricity, provide heat, and even facilitate seasonal storage.

During the formation of the Earth, materials from supernovas were expelled into space, including a wide range of elements, from lightweight to heavy atoms. These materials eventually formed clouds that collapsed due to gravitational forces, leading to the formation of planets. In the case of Earth, this process led to the accumulation of heavy materials at high temperatures, which persist to this day, releasing heat to the upper layers of the planet.

It is important to note that the structure of the Earth consists of multiple layers beneath the terrestrial crust, each with its own properties and characteristics resulting from the formation of rocks and geological processes that have occurred over time.

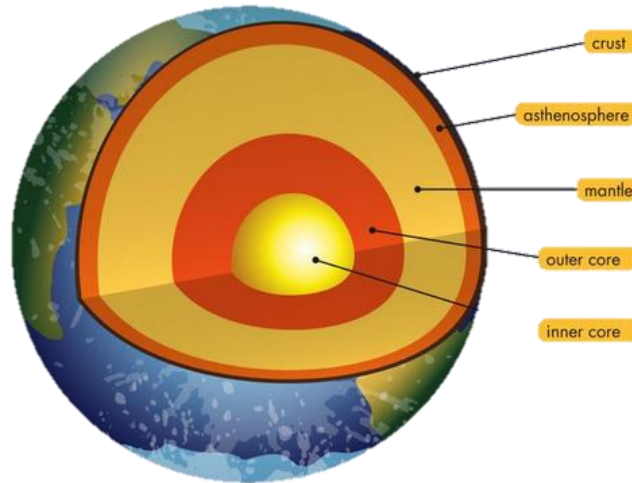


Illustration 2. Layers of the Earth. Eboch, M. M. (2019). Geothermal Energy. United Kingdom: Raintree Publishers.

Illustration 2 depicts the primary layers of the Earth, starting from the surface and extending to the core. The thickness of each layer is not precisely defined as it varies depending on the reference point on the planet's surface and the geological history of the region. Table 1 provides approximate estimated characteristics for each layer.

Layer	Thickness	Average temperature
Crust + lithosphere	100 km	500 °C
Asthenosphere	150 km	1355 °C
Mantle	2642 km	2770 °C
Outer core	2245 km	4410 °C
Inner core	1180 km	+ 5000 °C

Table 1. Thickness and average temperatures for different Earth's layers. Own adaptation from [6].

One noticeable observation is that the temperature increases with depth. However, the relationship between temperature and depth is not linear. It is estimated that the temperature gradient for the lithosphere layer is approximately 0.15 - 0.30 °C/km. This gradient is subject to tectonic movements, which cause variations in the gradient due to the continuous displacement of materials between upper and lower layers.

In terms of geothermal energy applications, it can be classified based on the resource's enthalpy, which is directly influenced by temperature. The classifications are as follows [7]:

- **Very low enthalpy system:** This refers to systems that operate at temperatures ranging from 5 to 25 °C and are associated with shallow volumetric spaces. These systems are particularly suitable for seasonal storage using heat pumps².
- **Low enthalpy system:** This type of system operates within the temperature range of 30 to 90 °C and utilizes water directly from geothermal wells. These systems can function with or without phase change, often leveraging the cavitation effect. They find applications in heating and residential climate control.
- **Medium enthalpy system:** Reservoirs with temperatures ranging from 90 to 150 °C fall under this category. The relatively higher temperature enables their use in household heating as well as electricity production through binary cycles.
- **High enthalpy system:** These sources are ideal for electricity generation, where temperatures exceeding 200 °C are required to drive a steam turbine. Various sub-systems are employed to maximize the utilization of residual energy before reinjecting it into the reservoir, such as binary cycles that employ isobutane or isopentane as the thermodynamic fluid.

2.1.3 Hydropower

Hydropower harnesses the potential energy of water at different heights to generate kinetic energy. This energy is utilized to drive turbines, which, in turn, power generators to produce electricity. Hydropower systems can vary in size and form, and two main types can be distinguished: impoundment facilities and run-of-river installations.

² An example of this is storing heat in summer to use it in winter.

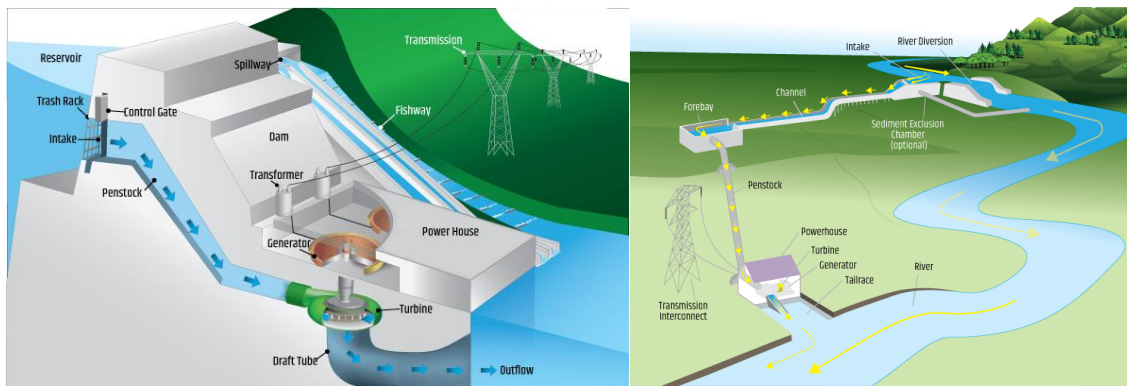


Illustration 3. Two main facilities for hydropower installations. Office of Energy Efficiency and Renewable Energy.

Impoundment facilities employ a dam to create a reservoir where water is stored. The water is then released through a penstock, which directs it to a turbine. This type of facility is typically used in larger-scale hydropower systems.

Run-of-river installations, on the other hand, utilize the natural flow of a river by diverting water through a channel to a powerhouse where it impels a turbine. This type of system is more suitable for low-energy generation.

A third category is a pumped storage facility, which shares similarities with an impoundment facility. However, it incorporates a pumping system that transfers water from a lower reservoir to an upper reservoir. This architecture allows the facility to absorb surplus energy from the grid during periods of low demand and store it in the upper reservoir. The stored water can then be released to generate electricity during periods of high demand, effectively serving as an energy storage tank.

2.1.4 Photovoltaic energy

Photovoltaic (PV) energy is widely used and recognized in both residential and high-power applications. It relies on the sun as the primary energy source, where photons are generated through the fusion of hydrogen atoms, resulting in the formation of helium in the sun's core. These photons traverse through the various layers of the sun before being emitted into space. Some of these photons reach the Earth's surface, where solar modules capture and convert them into electricity, a process known as the photogeneration effect.

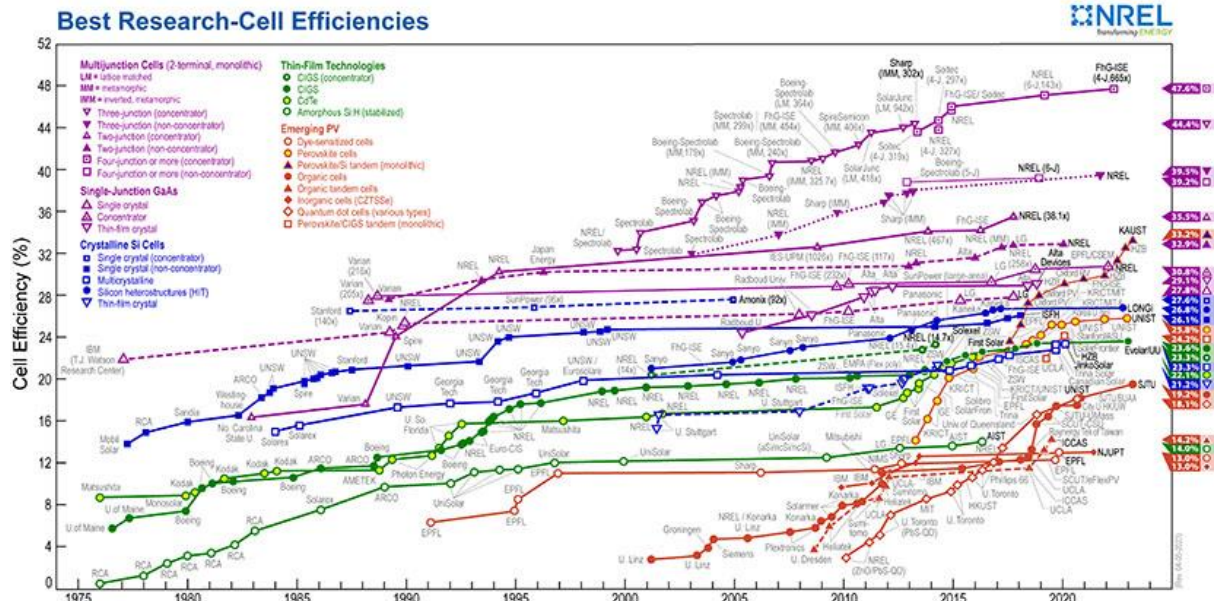


Illustration 4. Technologies and cell efficiencies developed. This plot is courtesy of the National Renewable Energy Laboratory, Golden, CO. 2023.

Illustration 4 provides an overview of different PV cell technologies, showcasing their historical development and the current efficiency status as of 2023. It is worth noting that commercial PV modules represent just one among several technologies depicted in the illustration. According to the latest reports, there are 26 types of cells classified into five major families [8].

- Multijunction cells
- Single-junction gallium arsenide cells
- Crystalline silicon cells
- Thin-film technologies
- Emerging photovoltaics

Table 2 (given below) shows the maximum efficiency reached by technology categorized by family, and year of the test. All these values have been evaluated in laboratory conditions according to IEC 60904-3, the standard test conditions are given for a cell at a temperature of 25 °C, irradiance of 1000 W/m², and for a spectral distribution AM1.5.

Family	Semiconductor	Highest efficiency	Year
Multijunction cells	Three-junction with concentration	44.40%	2013
	Three-junction without concentration	39.46%	2021
	Two-junction with concentration	35.50%	2017
	Two-junction without concentration	32.90%	2020
	Four-junction (or more) with concentration	47.60%³	2022
	Four-junction (or more) without concentration	39.20%	2019
Single-junction gallium arsenide cells	Single crystal	27.40%	2015
	Concentrator structure	30.80%	2022
	Thin-film crystal	29.10%	2018
Crystalline Si cells	Single crystal with concentration	27.60%	2007
	Single crystal without concentration	26.10%	2018
	Multicrystalline	24.40%	2020
	Silicon heterostructures	26.81%	2022
	Thin-film crystal	21.24%	2014
Thin-film technologies	CIGS ⁴ with concentration	23.30%	2014
	CIGS without concentration	23.60%	2023
	CdTe ⁵	22.10%	2015
	Amorphous Si:H ⁶	13.00%	2015
Emerging PV	Perovskite cells	25.80%	2022
	Perovskite/Si tandem	33.20%	2023
	Organic	19.20%	2023
	Organic tandem	14.20%	2019
	CZTSSe ⁷	13.00%	2021
	Dye-sensitized	13.00%	2020

³ It is the highest efficiency reached for a single technology; test was performed in Fraunhofer Institute for Solar Energy System's facility.

⁴ Copper Indium Gallium Selenide.

⁵ Cadmium Telluride.

⁶ Hydrogenated Amorphous Silicon.

⁷ Copper Zinc Tin Sulphur-Selenide

Quantum dot	18.10%	2020
Perovskite/CIGS tandem	24.20%	2020

Table 2. Highest efficiencies by cell technology. Own adaption from [8].

Photovoltaic effect

The photovoltaic effect is a fundamental process in solar cells, where photons are absorbed by a substrate material. Table 2 provides information on various substrates and architectures used in solar cell construction. The most common material in commercial applications is silicon, which is a semiconductor. The silicon is doped with boron or gallium to create a p-type semiconductor⁸, or with phosphorus or arsenic to create an n-type semiconductor⁹.

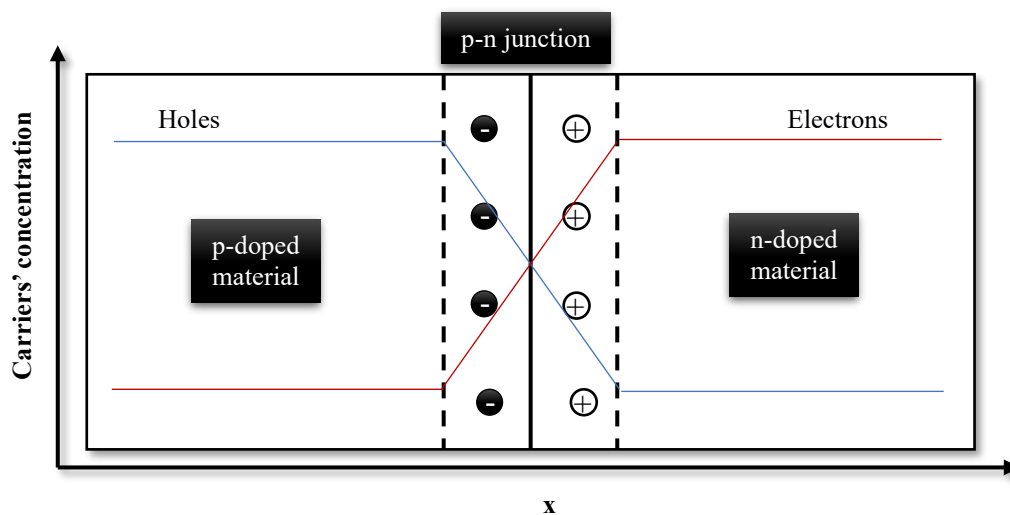


Illustration 5. p-n junction and carriers' concentrations.

Illustration 5 depicts a p-n junction formed by both the n-type and p-type semiconductors. This junction creates a region where there is an excess of holes and electrons, allowing for diffusion and recombination to occur, resulting in an electrically stable zone. This structure forms the basis of a solar cell as well as diodes. To better understand the functioning of a solar cell or a solar panel, it is necessary to introduce the concept of valence and conduction bands, as well as the concept of a forbidden band.

- **Valence band:** Refers to the outermost electron orbital of an atom, representing the highest energy level where electrons reside. It plays a

⁸ It can be called “electron acceptor” due to the capability to receive electrons on their electronic configuration.

⁹ Depending on literature, it can be called “electron donor” due the excess of electrons on their electronic configuration that allow to share easily.

crucial role in chemical reactions as electrons are shared and participate in bonding, influencing the atomic behaviour.

- **Conduction band:** is a region outside the atom where electrons are not influenced by the attractive forces of the nucleus. Electrons in the conduction band have high mobility and can move freely within a crystalline structure, allowing for electrical conductivity.
- **Forbidden band:** also known as the forbidden energy gap, is the energy range between the valence and conduction bands where the probability of finding an electron is effectively zero. It provides information about the bonding strength between the valence band and the atom's nucleus. A larger forbidden band indicates greater isolation of the material, making it less conductive.

Understanding the concepts of the valence band, conduction band, and forbidden band is crucial for comprehending the behaviour of materials in solar cells and their ability to generate electricity through the photovoltaic effect.

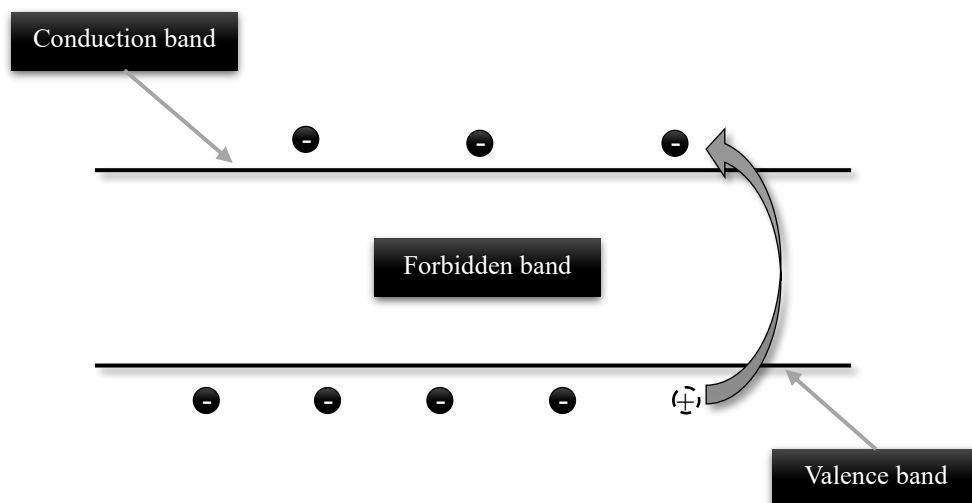


Illustration 6. Visual description of the different quantum bands.

When an electron in the valence band of a material absorbs energy, it can be excited to a higher energy state above the valence band. This causes the electron to "jump" from the valence band to the conduction band, which has a more suitable energy level for the electron. The reverse process also occurs, where an electron in the conduction band can lose energy and transition back to the valence band. Illustration 6 provides a visual representation of this phenomenon.

These previous paragraphs describe the fundamental physical mechanism of electron diffusion in a solar cell. In a semiconductor, such as silicon, the solar cell utilizes a p-n junction. When photons with sufficient energy strike the semiconductor, they can excite electrons, creating electron-hole pairs¹⁰. These pairs then diffuse through the semiconductor, eventually separating due to local electric fields. The electrons move towards the Electron Transport Layer (ETL), while the holes move towards the Hole Transport Layer (HTL) until they reach their respective collectors, thus completing the electrical circuit.

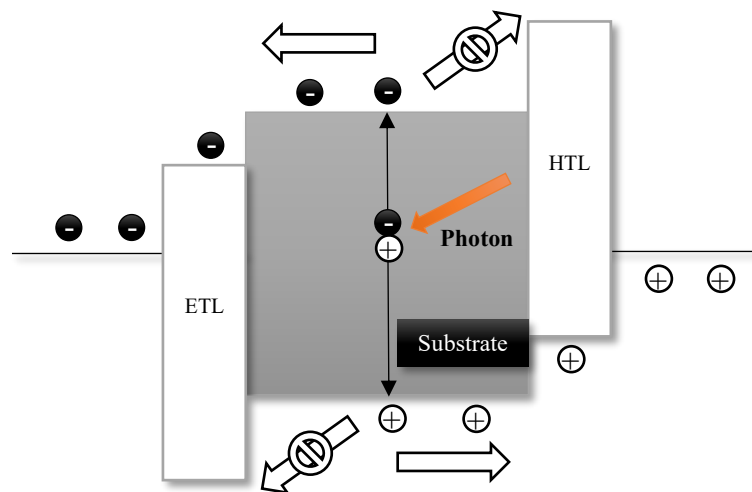


Illustration 7. Simplified band diagram considering ETL and HTL.

Illustration 7 showcases the main architecture of a solar cell, where the ETL and HTL act as conductors for electrons and holes, respectively. These layers function as filters, preventing the crossing of electrons (in the case of the HTL) and holes (in the case of the ETL) to lower energy states where recombination could occur. Such materials improve the efficiency of the solar cell by minimizing recombination losses.

Electrical parameters

In addition to the physical aspects of energy production, there are several electrical parameters that are used to evaluate the performance of a solar cell:

- **Reverse saturation current density [J_o]:** This parameter represents the current per unit area that would flow through the solar cell under reverse bias in complete darkness. It is determined by the intrinsic characteristics of the semiconductor material.

¹⁰ For each free electron formed, a hole is created as well.

- **Photocurrent density [J_{ph}]**: This parameter represents the current per unit area obtained when the solar cell is illuminated. It is the result of the absorption of photons and the generation of electron-hole pairs in the semiconductor.
- **Short circuit current density [J_{sc}]**: This parameter represents the current per unit area of the solar cell when the voltage between its terminals is zero. It is equal to the photocurrent generation and is influenced by factors such as temperature and incident radiation.
- **Maximum current density [J_{max}]**: This is the maximum current per unit area that a solar cell can provide under its maximum efficiency operating conditions.
- **Open voltage circuit [V_{oc}]**: This is the voltage between the positive and negative terminals of the solar cell when it is operating under its maximum efficiency conditions, with no external load connected. It depends on factors such as the solar cell temperature, short circuit current, and reverse saturation current density.
- **Maximum voltage [V_{max}]**: This is the maximum voltage that a solar cell can reach under its maximum efficiency operating conditions.
- **Fill factor [FF]**: The fill factor is a dimensionless parameter that represents the ratio between the area enclosed by the current-voltage (I-V) curve at maximum power point and the area enclosed by the I-V curve at the open circuit voltage and short circuit current. It provides information about the quality of the solar cell and its ability to deliver power.

$$FF = \frac{V_{max}J_{max}}{V_{oc}J_{sc}} \quad \text{Eq. 1}$$

- **Efficiency [η]**: The efficiency of a solar cell is a measure of how effectively it converts incident radiation into electrical energy. It is calculated by considering factors such as the fill factor, open circuit voltage, short circuit current, incident irradiance, and the solar cell temperature. It represents the ratio of the electrical power output to the incident power input.

$$\eta = \frac{FF \cdot V_{oc}J_{sc}}{P_{light}/A_{cell}} \quad \text{Eq. 2}$$

These electrical parameters help in assessing and comparing the performance of solar cells and understanding their conversion efficiency and power generation capabilities.

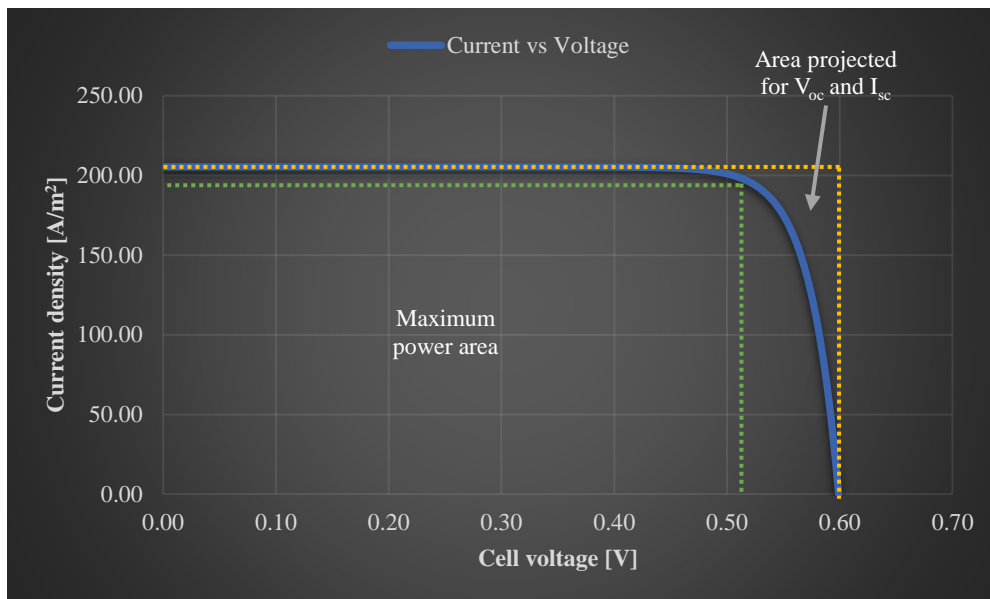


Illustration 8. Fill factor for a single solar cell.

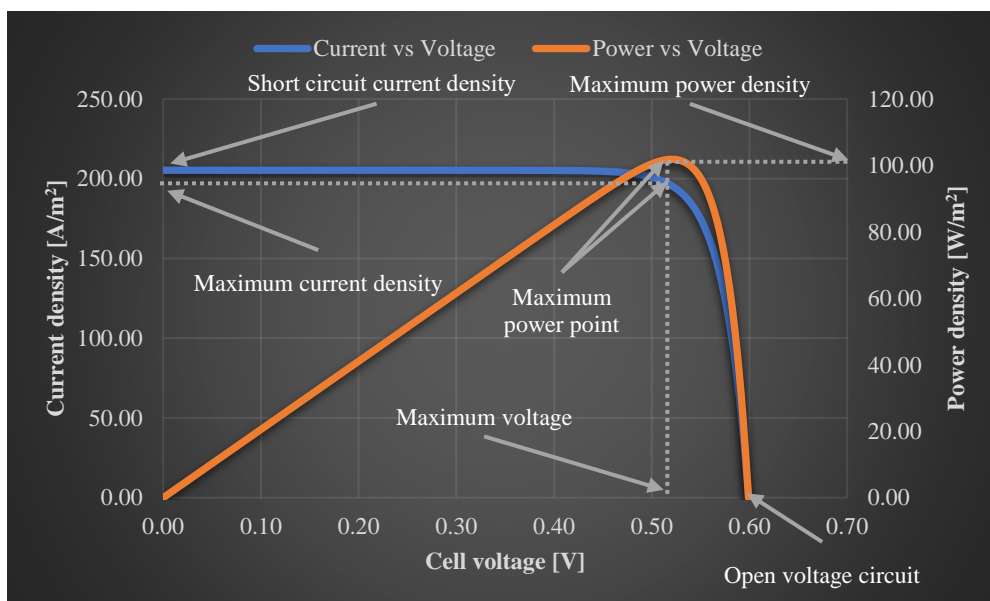


Illustration 9. Current and power density vs cell voltage for an ideal solar cell.

Illustration 8 and Illustration 9 depict the main parameters described earlier in the context of a solar cell's current-voltage (I-V) characteristics. It is important to note that the maximum power point does not necessarily correspond to the extreme values of voltage and current density individually, but rather represents the optimal combination of voltage and current density that results in the maximum power output for a given set of conditions.

The I-V curve of a solar cell shows the relationship between the voltage across the cell and the current flowing through it. The curve is influenced by factors such as temperature and incident irradiation, which can cause variations in the curve shape and the position of the maximum power point.

Illustration 8 illustrates the I-V curve of a solar cell under different operating conditions, showing how changes in temperature and irradiation affect the curve. The position of the maximum power point on the curve shifts with variations in these parameters.

Illustration 9 by other hand, focuses specifically on the maximum power point on the I-V curve. It highlights that the maximum power point is not a fixed point but varies with changing conditions. It is represented as a red dot on the curve and corresponds to the combination of voltage and current density that yields the maximum power output for the specific conditions.

These illustrations emphasize that the maximum power point of a solar cell is not a static value but rather depends on the prevailing operating conditions. Monitoring and optimizing the operating point of a solar cell to track the maximum power point under varying environmental conditions are important for achieving the highest possible power conversion efficiency and overall performance.

Ideal and real solar cell's electric circuit

In contrast to the simplified ideal solar cell model, the real solar cell model incorporates additional elements to account for practical considerations and the influence of various factors. These factors include the construction and manufacturing processes of the solar cell, as well as material defects that can affect its performance.

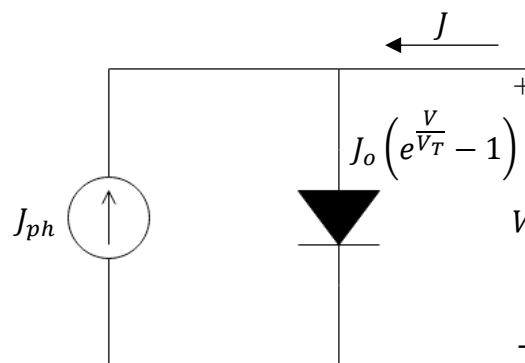


Illustration 10. Ideal solar cell equivalent circuit model.

$$J = J_o \left[e^{\left(\frac{V}{V_T}\right)} - 1 \right] - J_{ph} \quad \text{Eq. 3}$$

The real solar cell model includes additional components such as resistors, capacitors, and parasitic elements that capture the non-ideal behaviour of the device. These elements represent various losses and inefficiencies that are present in real-world solar cells.

For example, resistors are included to represent the series resistance and shunt resistance of the solar cell. Series resistance arises from the resistance of the conducting materials and interconnections within the cell, while shunt resistance accounts for leakage currents and bypass pathways that can reduce the cell's overall efficiency.

Capacitors are also incorporated to model the parasitic capacitances associated with the various layers and interfaces within the solar cell structure. These capacitances can affect the charge dynamics and response time of the device.

Furthermore, other non-ideal factors such as recombination losses, optical losses, and temperature effects are considered in the real solar cell model. These factors can have a significant impact on the overall performance and efficiency of the solar cell.

By incorporating these additional elements and considering the complexities of real-world conditions, the real solar cell model provides a more accurate representation of the behaviour of practical solar cell devices. It enables more comprehensive analysis and simulation of the cell's performance under various operating conditions and helps in optimizing its design and efficiency.

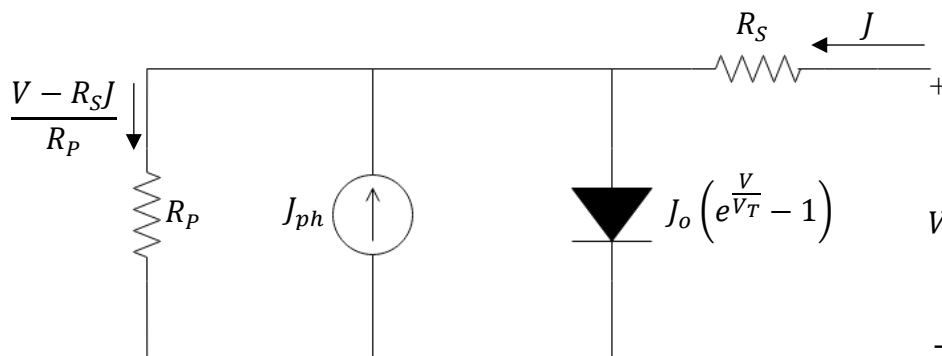


Illustration 11. Real solar cell equivalent circuit model.

$$J = J_o \left[e^{\left(\frac{V - R_S J}{nV_T} \right)} - 1 \right] + \frac{V - R_S J}{R_P} - J_{ph} \quad \text{Eq. 4}$$

In the real solar cell model, two additional parameters are introduced: series resistance and shunt resistance, which are represented as resistors in the equivalent circuit. The presence of these resistors for the non-ideal behaviour of the solar cell and introduces voltage drops and current deviations compared to the ideal model.

The series resistance reflects the response of the materials used in the solar cell to the flow of current. It causes a voltage drop across the cell due to the inherent resistance of the materials. The value of the series resistance can be determined experimentally by measuring the derivative of the current density with respect to voltage at low voltages and low illumination conditions.

On the other hand, the shunt resistance is related to manufacturing processes and represents alternative pathways for current flow in the solar cell. It causes a deviation of current density from the ideal behaviour. The shunt resistance value can be determined experimentally by measuring the derivative of the current density with respect to voltage at high voltages (near the bias voltage) and high illumination conditions.

Another parameter that is often considered in the real solar cell model is the ideality factor. It describes the extent to which the behaviour of the solar cell resembles that of an ideal diode, as predicted by theory [9]. An ideal solar cell would have an ideality factor of 1. However, in practical cases, the ideality factor typically does not exceed 2. If the ideality factor deviates significantly from these values, further investigation is required as it indicates a departure from classical transport mechanisms associated with the junctions. The ideality factor can be determined by analysing the dark current density equation, simplifying it by neglecting certain terms and isolating the expression for the ideality factor.

Solving the real solar cell model with these additional parameters becomes more complex due to the interdependence of current density, voltage, and the parallel resistance and diode branch. Numerical methods are often employed to solve the equations and analyse the behaviour of the real solar cell under different operating conditions.

$$n = \frac{qV}{kT \ln\left(\frac{J}{J_o}\right)} \quad \text{Eq. 5}$$

In both the ideal and real solar cell models, there are common elements: the photocurrent density and the dark current density.

The photocurrent density represents the current generated by the solar cell when it is illuminated by solar radiation. This current is produced as a result of the photogeneration effect, where photons are absorbed by the semiconductor material, exciting electrons from the valence band to the conduction band. The photocurrent density is a key parameter that determines the power output of the solar cell.

On the other hand, the dark current density is the current generated by the solar cell due to thermal excitation, even in the absence of illumination. This current arises from the movement of thermally excited charge carriers within the semiconductor material. The dark current density is typically small compared to the photocurrent density and is mainly influenced by factors such as temperature and material properties.

Regardless of the specific circuit model used, the reverse saturation current density and photocurrent density can be determined based on the dimensions and characteristics of the solar cell. In the case of a short solar cell with a passivated surface, these current densities can be quantified and analysed.

These common elements, the photocurrent density and dark current density, are fundamental for understanding the operation and performance of both ideal and real solar cells, and they play a crucial role in determining the overall efficiency of the solar cell.

$$J_o = q \frac{D_n}{W_p} n_o \cdot \frac{S_f}{S_f + \frac{D_n}{W_p}} + q \frac{D_p}{W_n} p_o \cdot \frac{S_b}{S_b + \frac{D_p}{W_n}} \quad \text{Eq. 6}$$

$$J_{ph} = \frac{1}{2} qG \left(W_p \cdot \frac{\frac{S_f}{\frac{D_n}{W_p}} + 2}{\frac{D_n}{W_p} + 1} + W_n \cdot \frac{\frac{S_b}{\frac{D_p}{W_n}} + 2}{\frac{D_p}{W_n} + 1} \right) \quad \text{Eq. 7}$$

2.1.5 Solar thermal energy

Solar thermal energy harnesses the thermal energy from the Sun's photons, rather than converting it directly into electricity like photovoltaic technology. Solar thermal technology has a wide range of practical applications, ranging from simple cooking devices to high-energy generation systems. In residential settings, solar thermal installations are commonly used for space heating and providing hot water.

Radioactive spectrum

When designing a solar thermal collector, it is important to consider not only the orientation and slope of the collector but also other factors such as the radioactive spectrum, selective materials, and fluid distribution within the system.

The radioactive spectrum refers to the distribution of wavelengths emitted by a body. While the Sun emits radiation across a broad range of wavelengths, not all of them are equally useful for thermal applications. In the context of solar thermal energy, the mid and long wavelengths of the electromagnetic spectrum, including the visible spectrum and infrared radiation, are particularly relevant.

Selective materials are used in solar thermal collectors to optimize the absorption of radiation in the desired wavelengths while minimizing losses in other wavelengths. These materials have properties that allow them to efficiently absorb and convert solar radiation into thermal energy.

Fluid displacement and distribution play a crucial role in solar thermal systems. Heat-absorbing fluids, such as water or specialized heat-transfer fluids, circulate through the collector, absorbing the thermal energy and carrying it to a storage or utilization system. Proper fluid displacement and distribution are important for maximizing the efficiency of the system and ensuring effective heat transfer.

By considering these factors, along with the orientation and slope of the collector, solar thermal systems can effectively capture and utilize the thermal energy from the Sun, providing a sustainable and renewable source of heat for various applications.

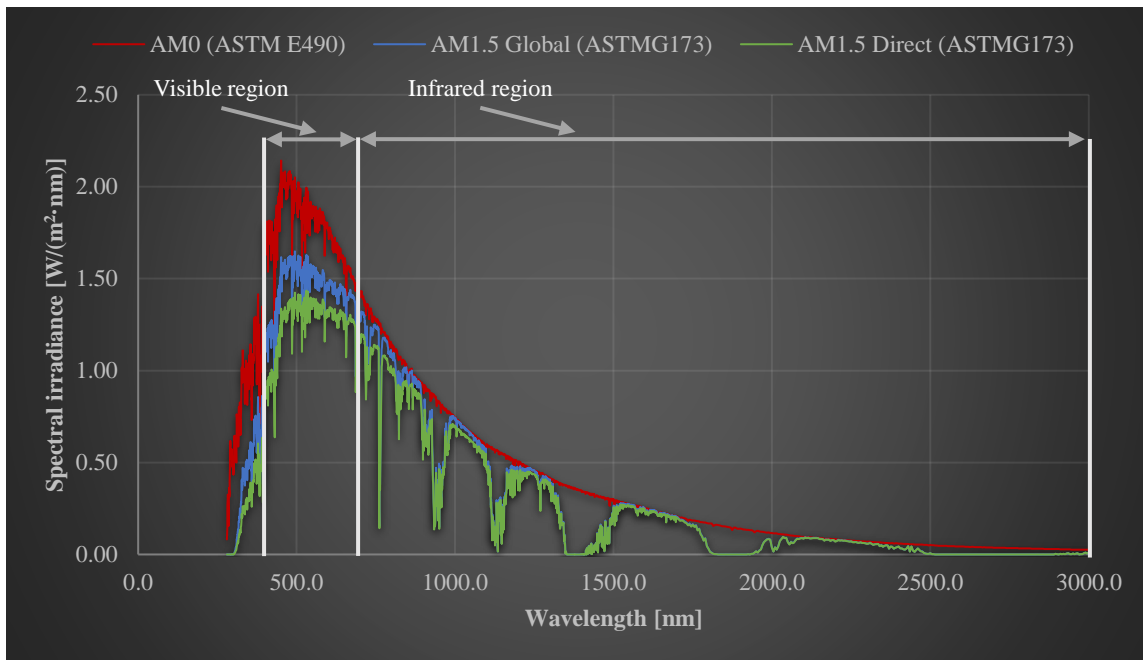


Illustration 12. Standard solar spectrum at different conditions. Data is courtesy of the National Renewable Energy Laboratory, Golden, CO.

Illustration 12 provides the spectral irradiance profiles under different conditions. The red curve represents the spectral irradiation for the outermost layer of the atmosphere, according to the ASTM E490 norm, which includes the *Standard Solar Constant and Zero Air Mass Solar Spectral Irradiance Tables*. The blue and green curves correspond to the ASTM G173 norm, which provides *Standard Tables for Reference Solar Spectral Irradiances* at ground level. The blue curve represents the overall spectrum, capturing all light components, while the green curve represents the direct beam of light.

In terms of useful band gaps for solar thermal applications, two main ranges are relevant: the visible spectrum and the infrared spectrum. The visible spectrum spans from approximately 400 to 700 nanometres (nm), while the infrared range extends from 700 nm to 10 micrometres (μm). Combined, these two ranges cover a significant portion of the solar spectrum.

To quantify this, approximately 42.21% of the total solar spectrum falls within the visible range, and 50.96% falls within the infrared range. This means that by utilizing both the visible and infrared spectrum, it is possible to take advantage of approximately 93.17% of the total available solar energy. This highlights the

importance of capturing radiation across a broad range of wavelengths in solar thermal systems to maximize energy absorption and conversion.

Radiant characteristics of materials

For a solar collector, the radiant characteristics of materials play a crucial role in optimizing energy absorption and minimizing thermal losses. Here are some important concepts related to these characteristics.

Black body: A black body is a theoretical concept that can absorb and radiate thermal energy at all wavelengths perfectly, according to Planck's law. It serves as a reference for comparing the radiative behaviour of real materials.

Emissivity: Emissivity refers to the fraction of thermal energy radiated by a real body compared to the energy radiated by an equivalent black body. It quantifies the material's ability to emit thermal radiation.

Absorptivity: Absorptivity is the fraction of incident energy that is absorbed by a material, leading to a change in its thermodynamic state. It represents the material's capacity to absorb incoming solar radiation.

Transmissivity: Transmissivity is the fraction of incident energy that passes through a material without significant thermal interaction. It does not necessarily mean that the energy's direction is unchanged inside the material.

Reflectivity: Reflectivity refers to the fraction of incident energy that interacts with the surface of a material and changes its direction, with at least one component being normal to the surface. It represents the material's ability to reflect incoming radiation.

These concepts are particularly important when considering the energy conservation law for incident charged particles. The energy of the charged particle must comply with this law, which ensures that energy is conserved during interactions with the material.

Understanding these radiant characteristics helps in selecting suitable materials for solar collectors that can effectively absorb solar energy while minimizing thermal losses through emission, transmission, or reflection.

$$\rho + \alpha + \tau = 1$$

Eq. 8

Where ρ , α , and τ are the reflectivity, absorptivity, and transmissivity. The behaviour of a material towards each mechanism depends on its specific conditions and properties.

For opaque materials, there may be certain wavelengths or ranges of wavelengths for which the material is not transparent, meaning that particles carrying energy at those wavelengths cannot pass through it. Instead, the material absorbs or reflects the energy. In this case, transmission becomes negligible for those wavelengths.

Opaque materials are typically designed to have high absorptivity and low transmissivity for the wavelengths of interest. This allows them to efficiently absorb solar radiation and convert it into thermal energy without significant loss through transmission.

Understanding the behaviour of materials with respect to absorption, transmission, and reflection is important in designing solar collectors that can effectively harness solar energy and optimize its conversion into usable thermal energy.

Low and medium temperature collectors

In the case of low and medium temperature solar collectors, the design and sizing depend on several factors. One important consideration is the thermal absorption capacity of the collector, which determines the amount of energy it can capture. On the other hand, the design also takes into account the specific requirements of the installation, such as water flow rate and the desired temperature in the system. This includes considering losses that may occur through tubes, pipes, storage tanks (if applicable), and other accessories.

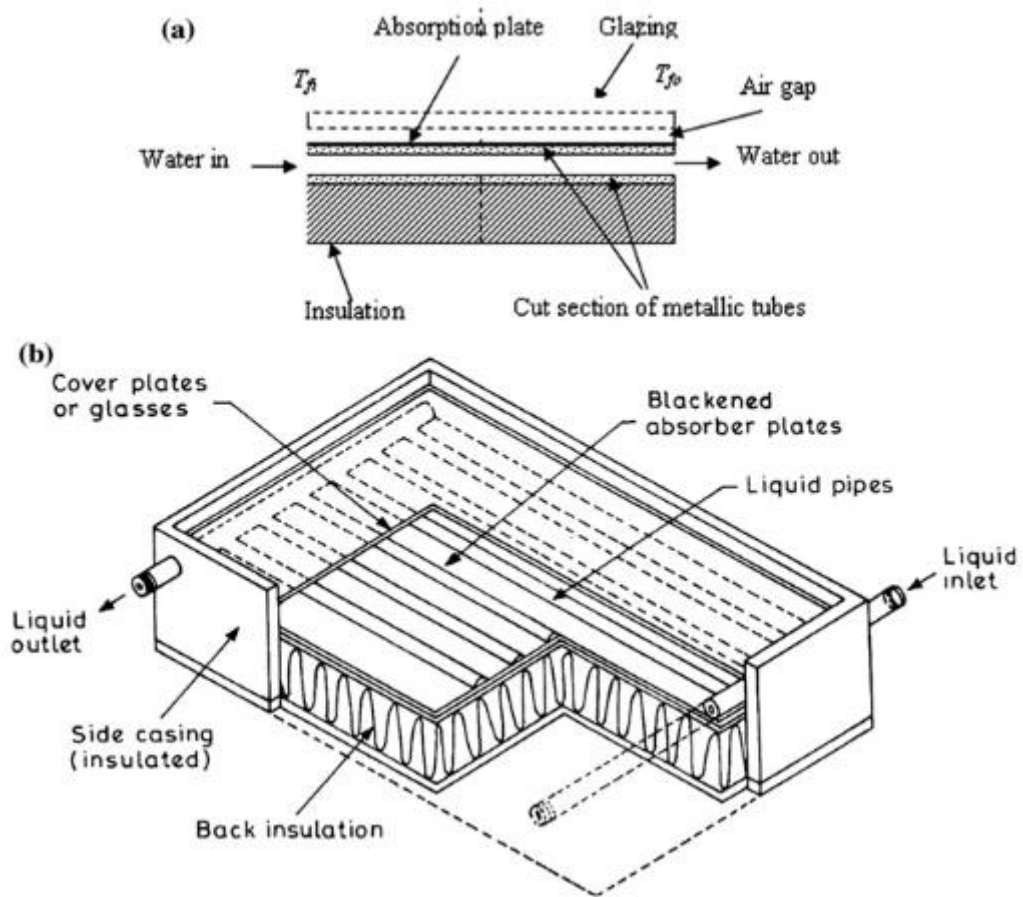


Illustration 13. Main components for a flat plate collector [10].

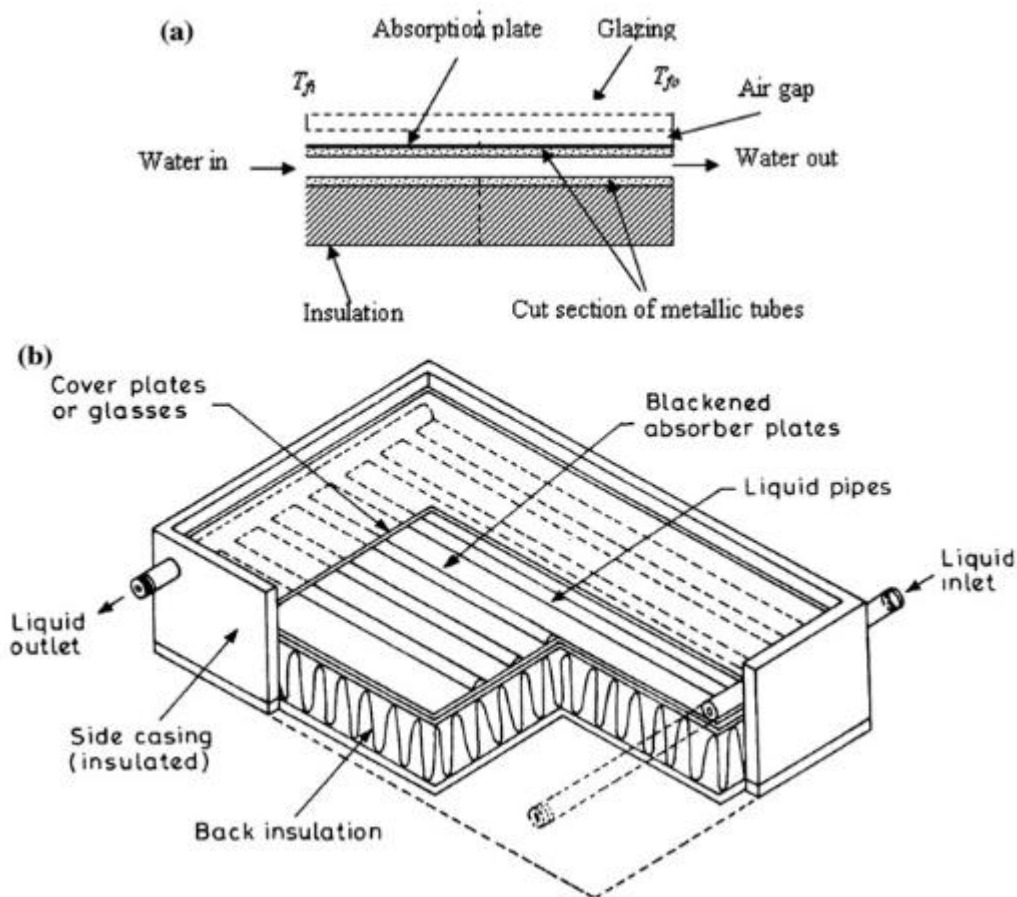


Illustration 13 depicts a basic flat plate collector, which is a commonly used design. The top of the collector is typically covered with glass plates that allow short wavelengths (visible light) to pass through while minimizing reflection. The cover should also be opaque to long wavelengths (infrared) to prevent excessive heat loss. Depending on the application and desired temperature increase, flat plate collectors can be single-layered, double-layered, or equipped with multiple cover plates.

The absorbing plate, located beneath the cover, is made of selective materials. These materials have high absorption properties for short wavelengths (allowing efficient conversion of photons into heat) and low emissivity for longer wavelengths (reducing the radiation of excess heat to the surroundings). The absorbing plate is responsible for capturing solar energy and raising its temperature within the collector.

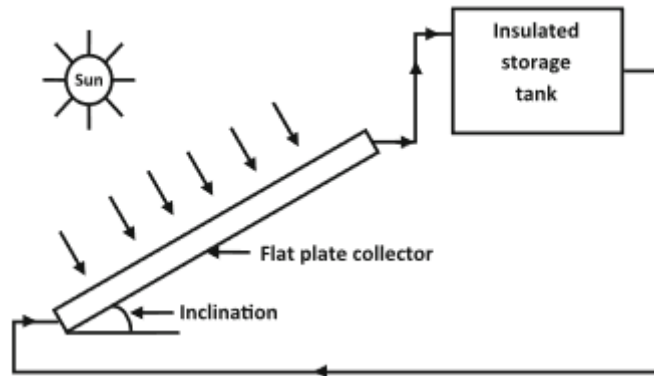


Illustration 14. Mainly flow direction in a flat plate collector with a storage tank [10].

In a typical flat plate collector, internal tubes are used to contain the working fluid, which is usually water in most applications. These tubes are in direct contact with the absorbing plate, allowing thermal energy to be transferred from the plate to the fluid through conduction. The fluid then carries the heat away from the collector.

Illustration 14 illustrates the typical fluid direction within a flat plate collector. The working fluid enters the collector from one end, flows through the internal tubes, and exits from the other end. This flow pattern ensures efficient heat transfer between the absorbing plate and the fluid. In some installations, a pumping system is employed to create turbulent flow within the tubes. This turbulent flow improves the heat transfer rate and enables the fluid to be delivered to the desired location or application.

Alternatively, a thermosyphon unit can be used, which operates based on natural convection. In a thermosyphon system, the fluid circulation is driven by density differences caused by temperature variations. As the fluid is heated by the absorbing plate, it becomes less dense and rises, creating a natural flow. The heated fluid then moves upward, transferring heat to the desired location, and eventually cools down and flows back to the collector due to gravity. Thermosyphon systems do not require a separate pumping system, as the fluid circulation occurs naturally.

Efficiency curve and heat absorption

The evaluation of energy heat transfer in a flat plate collector involves performing an energy balance for each component within the collector. These components include the cover plate, collector, lateral walls, isolated base, absorber, and internal tubes. The energy balance takes into account the geometric dimensions and material properties of each component, which are represented by a global heat transfer coefficient U_L .

The global heat transfer coefficient U_L represents the overall heat transfer characteristics of the collector. It combines the individual heat transfer coefficients of each component, taking into consideration their surface areas, thermal conductivities, and convective heat transfer coefficients. By incorporating U_L into the energy balance equations, the heat transfer from the collector to the fluid can be calculated.

In addition to the heat transfer within the collector, the energy balance also considers the fluid gains. This involves evaluating the heat absorbed by the working fluid as it passes through the internal tubes in contact with the absorber. The inlet water temperature is a known parameter for these calculations.

By performing energy balances for both the collector components and the fluid gains¹¹, the overall efficiency of the flat plate collector can be determined. The efficiency curve of the collector shows the relationship between the absorbed solar heat and the incident solar radiation for different operating conditions, such as fluid flow rate and inlet temperature. This curve provides insights into the performance of the collector and helps in optimizing its design and operation.

$$F_R = \frac{\dot{m}C_p(T_{fo} - T_{fi})}{A_c[I_\alpha - U_L(T_{fi} - T_a)]} \quad \text{Eq. 9}$$

Where F_R is related to the removal factor that can be interpreted as the effectiveness of the flat plate collector and indicates the ratio of actual heat transfer and maximum heat transfer at same conditions. This equation takes into account the collector's effectiveness, the heat transfer characteristics of the collector components, the surface area of the collector, and the incident solar radiation. The product of the

¹¹ It is evaluated conduction, convection and radiation gains and losses across the material.

equivalent transmissivity and absorptivity represents the portion of solar radiation absorbed by the collector.

By calculating the efficiency using this equation, the performance of the flat plate collector can be assessed and compared under different operating conditions and design parameters. It provides a measure of the collector's ability to convert incident solar radiation into useful thermal energy.

$$\eta = F_R(\tau\alpha) - F_R U_L \frac{(T_{fi} - T_a)}{I} \quad \text{Eq. 10}$$

Eq. 10 is specific for each flat plate collector. The left term represents the maximum theoretical efficiency achievable based on the design and material selection of the collector. The right term accounts for various losses, such as conduction, convection, and radiation losses, which can reduce the actual efficiency of the collector.

It is important to consider that the efficiency equation may have additional factors or terms specific to the particular flat plate collector being analysed. The design, materials, and operating conditions of the collector can impact the equation and the resulting efficiency calculation.

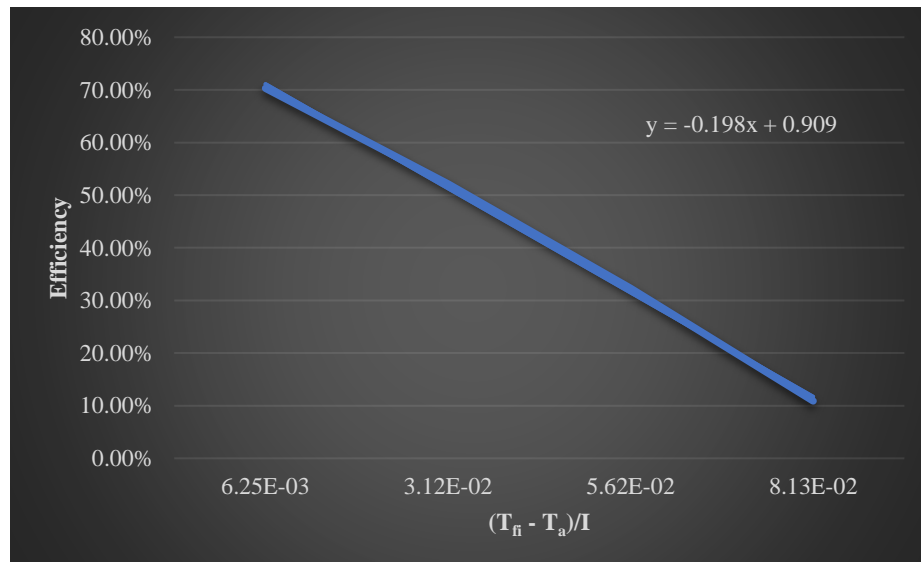


Illustration 15. Typical efficiency curve for a flat plate collector.

Illustration 15 shows an example of a collector efficiency curve, which is typically represented as a linear plot. The negative slope of the curve represents the

losses in the collector. The theoretical maximum efficiency, in this case, is approximately 91%.

The term "0.198" represents the product of F_R (removal factor) and U_L (overall heat transfer coefficient). This term is used to account for the losses in the collector and is specific to the design and characteristics of the collector being analysed.

By examining the collector efficiency curve, one can determine the actual efficiency of the collector at different operating conditions and compare it to the theoretical maximum efficiency. This information is valuable in evaluating the performance and effectiveness of the collector in converting solar energy into usable heat.

$$Q_u = \eta I A_c \quad \text{Eq. 11}$$

The useful energy absorbed by the collector can be calculated by multiplying the incoming solar energy, the collector surface area, and the efficiency of the device. This represents the amount of energy that is effectively captured and utilized by the collector for heat transfer purposes.

Another approach to evaluate the heat exchange in a collector is by considering the change in enthalpy of the fluid that flows through it. Enthalpy is a thermodynamic property that accounts for both the internal energy and the work done by or on the system. By measuring the change in enthalpy of the fluid before and after it passes through the collector, one can quantify the amount of heat energy that has been transferred to the fluid.

Both approaches provide valuable insights into the performance and effectiveness of the collector in converting solar energy into usable heat.

$$Q_u = \dot{m} C_p (T_{fo} - T_{fi}) \quad \text{Eq. 12}$$

Enthalpy change in Eq. 12 is based on the specific energy of the fluid and the temperature change. It does not explicitly take into account the structure of the collector, but rather focuses on the thermodynamic properties of the fluid itself.

By considering the specific energy (enthalpy) of the fluid and the temperature change it undergoes as it passes through the collector, one can determine the amount

of heat energy that has been absorbed by the fluid. This information is particularly useful for sizing the solar thermal installation and evaluating its performance in terms of heat transfer.

It is important to note that while the specific energy and temperature change are significant factors in determining the heat exchange, the overall efficiency of the collector should still be considered to assess the effectiveness of the system in converting solar energy into usable heat.

High temperature applications

In high-temperature applications, the focus is on concentrating sunlight to achieve higher temperatures and enable the phase change of a fluid, which can then be used to drive a generator through a steam turbine or a Stirling engine. Several technologies have been developed for high-temperature solar applications, including:

- **Parabolic trough collectors:** This technology uses parabolic mirrors to concentrate sunlight onto a receiver tube located at the focal point. The receiver tube contains a thermodynamic fluid such as water or oil, which absorbs the solar energy and transfers it for further use.

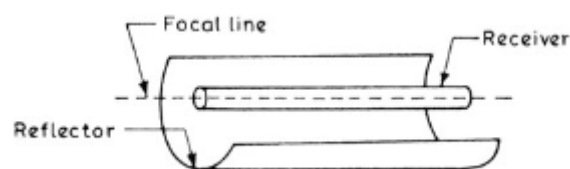


Illustration 16. View of parabolic trough collector [10].

- **Central solar receiver:** This technology involves a field of mirrors, also known as heliostats, that track the sun's movement and concentrate the sunlight onto a central tower. The concentrated solar energy is used to heat a fluid, typically molten salt, which can be stored and used to generate electricity or provide heat.

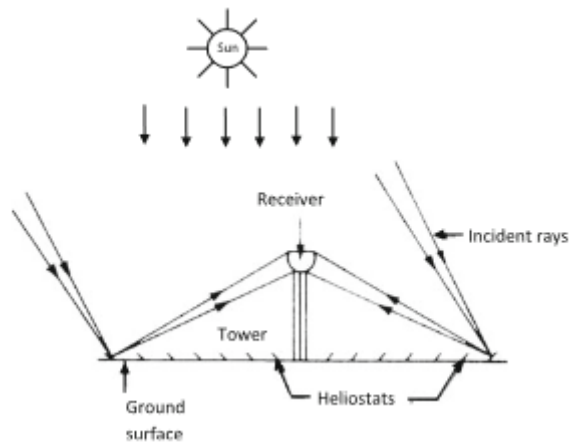


Illustration 17. Simplified scheme of a central solar receiver [10].

- Linear Fresnel lens:** Like parabolic trough collectors, linear Fresnel lens systems use flat or slightly curved mirrors to concentrate sunlight onto a receiver tube. The mirrors are arranged in a linear configuration, and the system typically requires tracking in only one axis. This technology offers cost advantages compared to parabolic troughs but may have lower overall efficiency.

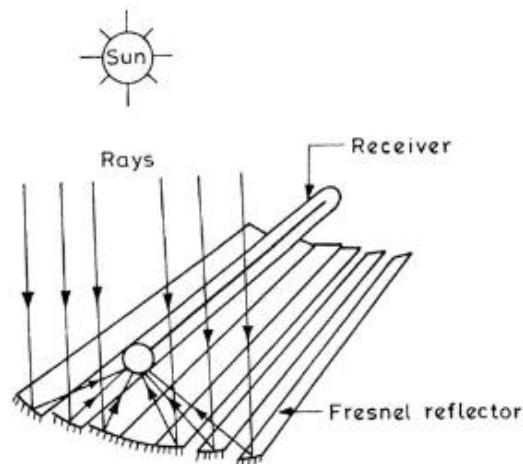


Illustration 18. Scheme of a Linear Fresnel [10].

- Parabolic dishes:** Parabolic dish systems use large, curved mirrors to focus sunlight onto a receiver located at the focal point. The receiver typically contains a Stirling engine, which converts the thermal energy into mechanical energy that can be used to generate electricity. Parabolic dishes require two-axis tracking to follow the sun's movement throughout the day.



Illustration 19. View of a parabolic dish [10].

Technology	Land Coverage	Efficiency	Installation Cost	Operation Cost	Solar Hours Required
Parabolic Trough Collectors	High	Relatively High	Moderate to High	Moderate	Moderate to High
Central Solar Receiver	Moderate to High	High	High	High	High
Linear Fresnel Collectors	Moderate	Moderate to High	Moderate to High	Moderate	Moderate to High
Parabolic Dishes	Low	Moderate to High	Moderate	Moderate	Moderate to High

Table 3. Comparison of main concentrated solar plant technologies [11].

As indicated in

Technology	Land Coverage	Efficiency	Installation Cost	Operation Cost	Solar Hours Required
Parabolic Trough Collectors	High	Relatively High	Moderate to High	Moderate	Moderate to High
Central Solar Receiver	Moderate to High	High	High	High	High
Linear Fresnel Collectors	Moderate	Moderate to High	Moderate to High	Moderate	Moderate to High
Parabolic Dishes	Low	Moderate to High	Moderate	Moderate	Moderate to High

Table 3, each high-temperature solar collector technology has its own set of characteristics. Parabolic trough collectors require a relatively high amount of land

coverage due to their large mirror surface area. However, they offer a relatively high annual efficiency, which helps to offset the installation costs. The operation costs are moderate, making it a viable option for certain applications.

Central solar receiver technologies, on the other hand, have a moderate to high land coverage requirement. They offer high efficiency and can produce a significant amount of energy. However, the installation and operation costs are generally high. Additionally, these technologies typically require a higher number of solar hours to generate the desired output, which can limit their applicability in certain regions.

Linear Fresnel collectors and parabolic dishes have a moderate land coverage requirement. They offer moderate to high efficiency and are technologies that are continuously improving. The installation and operation costs are generally in the moderate to high range, depending on the specific design and implementation.

Overall, the choice of technology depends on various factors, including the available land, desired efficiency, installation and operation costs, and the solar resource in a particular location. Each technology has its advantages and limitations, and ongoing advancements aim to enhance their performance and cost-effectiveness.

2.1.6 Tidal and wave power

Ocean energy has enormous potential due to the vast expanse of the world's oceans. The estimated potential for ocean energy is significant, ranging from 20,000 to 80,000 terawatt-hours (TWh), which could satisfy a substantial portion of global electricity demand. However, the current installed capacity is relatively low, at around 535 megawatts (MW), indicating the need for further development and investment. The goal is to increase the installed capacity to 100 gigawatts (GW) by 2050 [12] to harness the full potential of ocean energy.

One of the main challenges facing tidal and wave power is the cost of deployment and operation. These technologies require substantial upfront investment and face technical and logistical challenges due to their offshore nature. However, ongoing research and development efforts aim to improve efficiency, reduce costs, and make ocean energy competitive with other renewable energy sources.

By overcoming these challenges, tidal and wave power technologies have the potential to contribute significantly to the global energy mix, offering a clean and renewable source of electricity from the vast energy resources of the world's oceans.

Tidal power

Tidal power utilizes the natural rise and fall of ocean tides caused by the gravitational forces of the Moon and the Sun. Tidal power plants typically consist of barrages or tidal turbines installed in coastal areas. When the tide rises, water is allowed to flow into a reservoir, and as the tide falls, the water is released back to the sea, driving turbines to generate electricity. Tidal power plants can provide a consistent and predictable source of energy due to the regularity of tidal cycles.



Illustration 20. Rance Tidal Power Station [13].

Illustration 20 shows the Rance tidal power plant, located on the estuary of the Rance river in France, is indeed one of the notable examples of tidal power installations.

The Rance tidal power plant has a total installed capacity of 240 megawatts (MW), making it the second-largest tidal power plant in the world. It consists of 24 bulb turbines, each with a diameter of 5.35 meters, and a total length of 750 meters. The plant takes advantage of the tidal movements in the estuary to generate electricity.

The capacity factor of the Rance tidal power plant is approximately 40%. The capacity factor represents the actual electricity generation compared to the maximum possible generation if the plant operated at full capacity continuously. With this capacity factor, the Rance tidal power plant produces approximately 600 gigawatt-hours (GWh) of electricity per year.

In the context of France's electricity demand, the annual electricity production of the Rance tidal power plant covers approximately 0.012% of the country's total demand. While this may seem relatively small in percentage terms, it still represents a significant contribution to the renewable energy mix and helps reduce carbon emissions associated with conventional power generation.

The Rance tidal power plant serves as an important demonstration of the potential of tidal power as a viable renewable energy source. It has been operational since 1966, showcasing the long-term reliability and sustainability of tidal power technology.

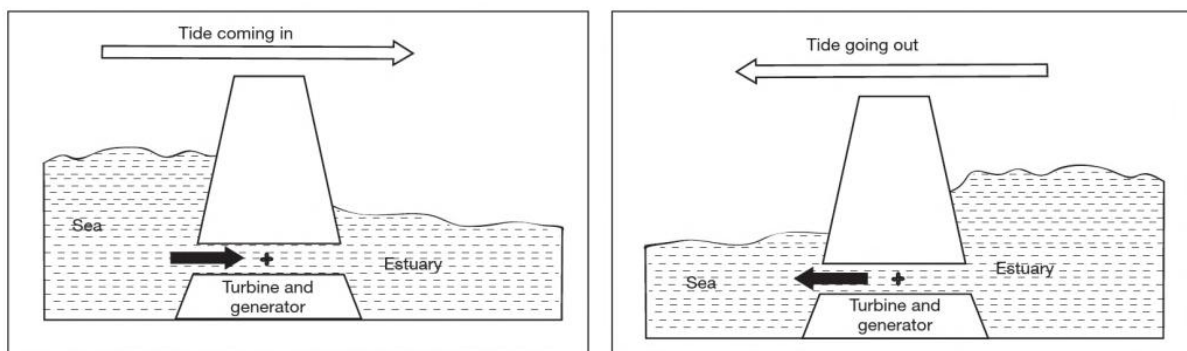


Illustration 21. Tidal power plant cross section view and water flow directions [14].

In

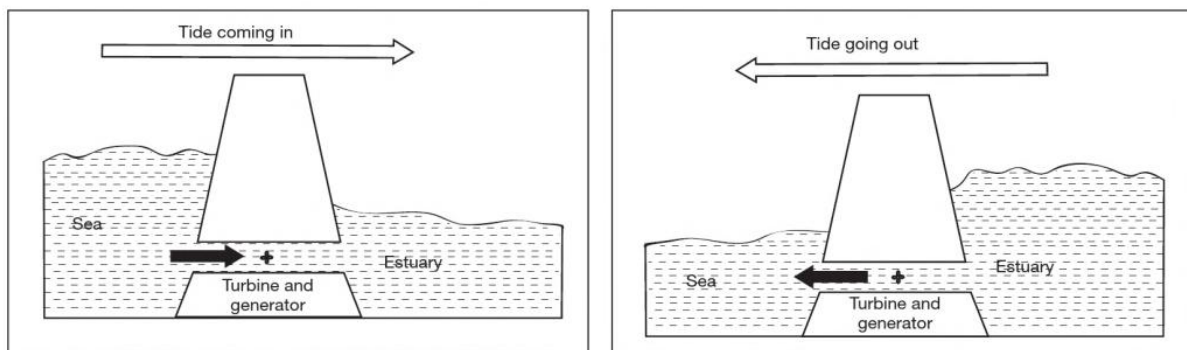


Illustration **21** depicts a typical installation for tidal power generation, showcasing the bidirectional water flow through the turbine. The illustration also highlights important features such as the tidal reference point, marked by a blue dashed line, and the two levels of water difference.

The first level difference, in the left-side illustration, represents the initial condition where the sea level is higher than the tidal basin's water level. This creates a gradient, and water flows from the ocean towards the tidal basin, moving from left to

right in the illustration. This influx of water is utilized to generate electricity as it passes through the turbine.

Conversely, the second level difference, showed in the right-side illustration, occurs when the water level in the tidal basin becomes higher than the sea level. In this situation, water flows from the basin back to the ocean, moving from right to left in the illustration. This outflow of water can also be harnessed to generate electricity as it passes through the turbine.

The tidal cycle is characterized by the continuous alternation between these two levels of difference, resulting in a cyclical movement of water and the generation of electricity during both inflow and outflow phases. This bidirectional flow allows for a consistent and continuous generation of tidal power as the tides rise and fall.

It's worth noting that the specific design and configuration of tidal power installations may vary, but the fundamental principle remains the same: harnessing the kinetic energy of water movement during tidal cycles to generate renewable electricity.

Wave power

Wave power technology captures the energy from ocean waves and converts it into electricity. There are different approaches to wave power generation, including oscillating water columns, point absorbers, and overtopping devices. These technologies vary in their mechanisms of capturing wave energy, but they all involve the movement of a device or structure in response to wave motion, which is then used to generate electricity. Wave power is still in the early stages of development and faces challenges related to the harsh marine environment and the variability of wave conditions.

- **Point absorber buoys:** These devices consist of a buoy anchored to the seabed that moves up and down with the waves. The vertical motion of the buoy is converted into linear motion, which drives a generator to produce electricity.

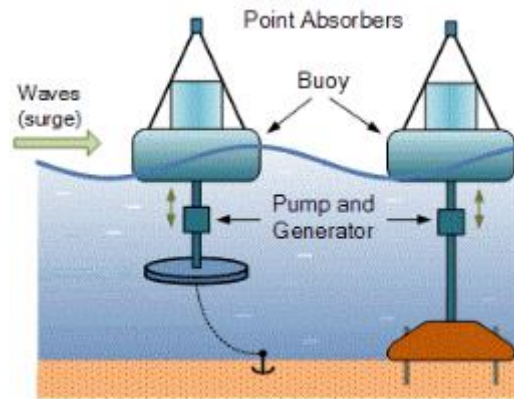


Illustration 22. Representation of a point absorber buoy [15].

- **Surface attenuators:** Surface attenuators operate parallel to the direction of the waves. They consist of interconnected modules that move relative to each other as the waves pass through. This relative movement is harnessed to generate electricity.

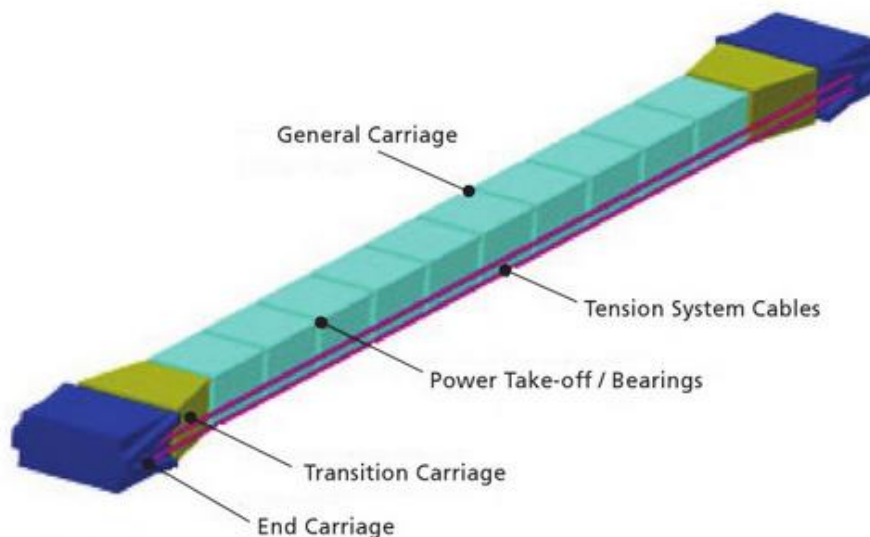


Illustration 23. Attenuator's main components [16].

- **Oscillating water columns:** Oscillating water columns do not directly use wave oscillations but rather utilize the air flow generated by pressure differences caused by wave action. They typically consist of a partially submerged chamber that is open to the ocean. As waves enter the chamber, the rising water level compresses the air inside, which then flows through a turbine to generate electricity. When the water level recedes, a vacuum is created, causing air to be drawn back into the chamber, which also drives the turbine.

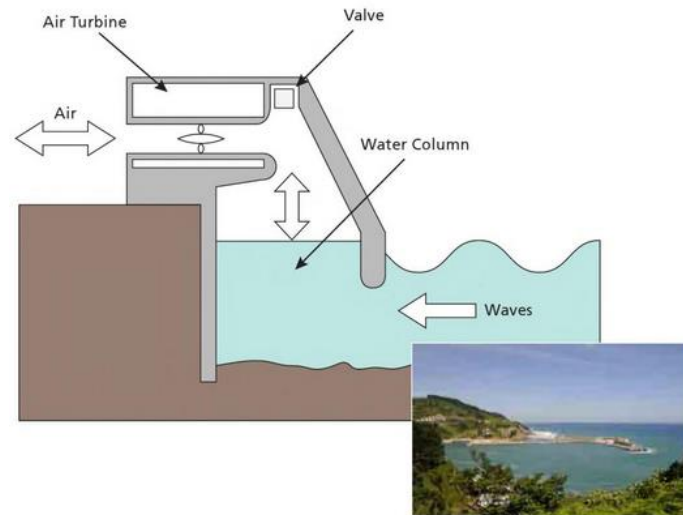


Illustration 24. Scheme of an oscillating water column device (left) and Mutriku Wave Power plant (right) [16].

- **Overtopping devices:** Overtopping devices are designed to capture the excess water that exceeds the overtopping level of a structure. The captured water is channelled into a reservoir and then directed through a penstock, where it drives a turbine to generate electricity.

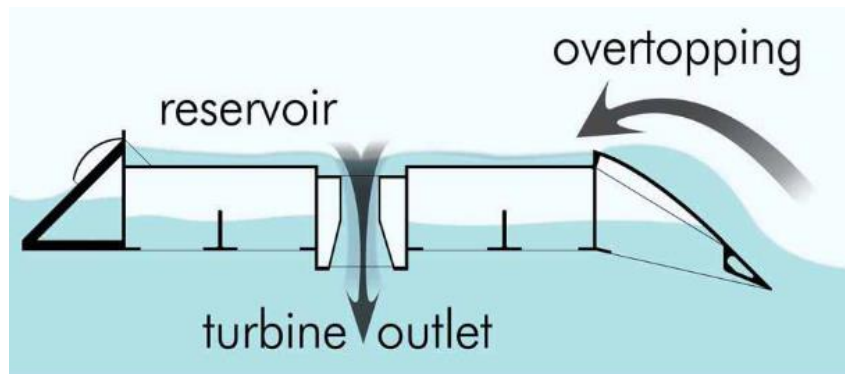


Illustration 25. Cross section of an overtopping device [17].

These different wave power technologies have varying degrees of maturity and deployment. Wave power is still in the early stages of development, and there are ongoing research and innovation efforts to improve efficiency, durability, and cost-effectiveness. The main challenges faced by wave power technologies include the harsh marine environment, variability of wave conditions, and the high costs associated with installation and maintenance.

2.1.7 Wind power

Wind power is a renewable energy source that harnesses the kinetic energy of wind and converts it into electricity. Wind energy is derived from the movement of air masses caused by temperature differences and global atmospheric circulation patterns. While wind power has the advantage of being an abundant and clean energy source, it is also unpredictable and variable, making it necessary to carefully assess wind resources for effective utilization.

There are different types of wind turbines used to capture the energy from wind:

- **Darrieus wind turbine:** This type of wind turbine belongs to the vertical-axis family. It typically consists of two or three vertical blades that are connected to a central axis. Darrieus turbines have the advantage of operating efficiently in various wind conditions. However, they suffer from drawbacks such as high ripple torque and stress on the central axis. To compensate for these issues, Darrieus turbines are often coupled with another type of turbine.

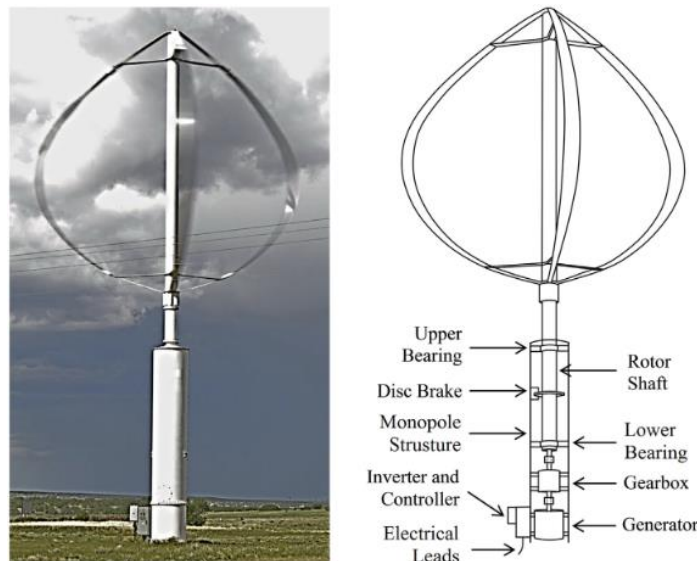


Illustration 26. A Darrieus wind turbine model VP100 (left), main components (right) [18].

- **Savonius wind turbine:** Is also a vertical-axis wind turbine. It is characterized by its S-shaped blades, which create drag as the wind passes over them. Savonius turbines are simple in design, low-cost, and can start rotating with low wind speeds. However, they have limited power and efficiency, making them more suitable for small-scale or remote applications, such as powering measurement devices or ventilation systems.

- **Horizontal wind turbine:** The horizontal-axis wind turbine (HAWT) is the most commonly used wind turbine design for both onshore and offshore installations. It consists of a rotor with three or more blades attached to a horizontal shaft. The rotor is mounted on top of a tower, and inside the tower, various mechanical, electrical, and control systems are housed in a nacelle. Horizontal wind turbines are known for their higher power output and efficiency compared to vertical-axis turbines. They can capture the wind from different directions and are suitable for utility-scale wind farms.

Wind power technology has seen significant advancements over the years, including improvements in turbine design, rotor efficiency, and control systems. Large-scale wind farms are being deployed worldwide, both onshore and offshore, to harness the power of wind and contribute to the global energy mix.

Wind turbine components

For a horizontal wind turbine, the main components typically include:

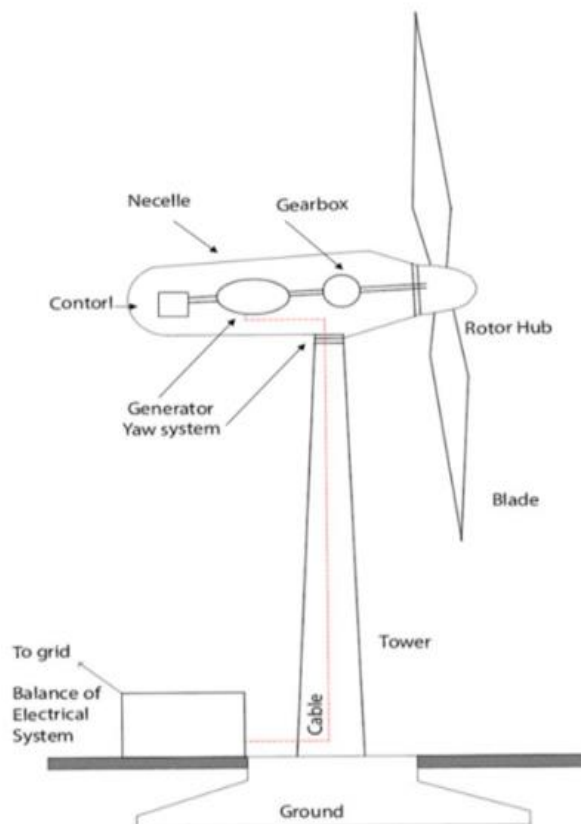


Illustration 27. Overall components of a horizontal wind turbine [19].

- **Foundation:** Provides a solid base for the wind turbine and is designed to withstand the vertical weight of the turbine and the bending stresses caused by wind forces. It also includes an underground wiring structure for interconnection between the turbine and the central control room.
- **Tower:** Is the tall structure that supports the wind turbine components. It provides elevation to capture higher wind speeds and allows for access to the nacelle and blades for maintenance and repair. The tower also houses the internal wiring system that connects the turbine components.
- **Nacelle:** Is the housing located at the top of the tower. It contains various components, including the generator, gearbox, and control systems. The nacelle protects these components from the environment and supports their operation.
- **Hub:** Is a central component in the nacelle that connects the rotor blades to the main shaft. It provides support for the blades and houses the pitch control system, which adjusts the angle of the blades to optimize energy capture and ensure safe operation.
- **Blades:** These are the aerodynamic elements of the wind turbine that capture the kinetic energy of the wind and convert it into mechanical rotation. The shape and profile of the blades are designed to maximize energy capture and provide aerodynamic efficiency. Typically, wind turbines have three blades, although some designs may have more.
- **Transformer:** Is responsible for converting the electrical power generated by the wind turbine from one voltage level to another. Depending on the wind turbine design, the transformer may be located in the nacelle or at the base of the tower. It ensures that the electricity generated by the turbine is compatible with the grid or can be efficiently transmitted over long distances.

These are the main components of a horizontal wind turbine, but there are also other auxiliary components such as yaw systems (to adjust the turbine's orientation with respect to the wind direction), anemometers (to measure wind speed), and various sensors and monitoring systems for performance and safety monitoring. The

specific configuration and design of these components may vary depending on the manufacturer and turbine model.

Wind energy

The wind power equation relates the power available in the wind to the properties of the wind flow. It can be expressed as:

$$P = \frac{1}{2} \rho A_b v^3 \quad \text{Eq. 13}$$

$$P_e = P\eta \quad \text{Eq. 14}$$

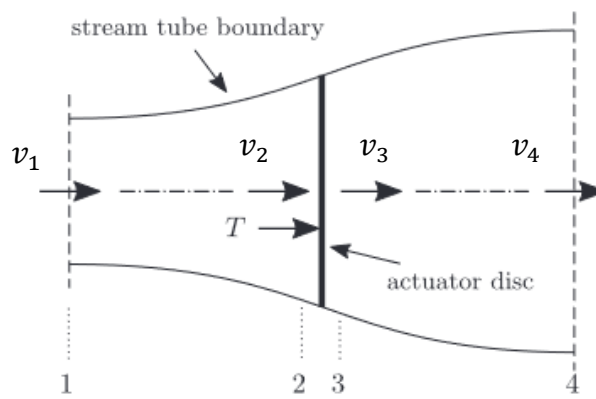


Illustration 28. One-dimensional projected conditions [20].

Eq. 13 shows that the power available in the wind is directly proportional to the air density, the swept area of the rotor blades, and the cube of the wind velocity. Therefore, even small changes in wind velocity can have a significant impact on the power output of a wind turbine.

The electrical power output (Eq. 14) of a wind turbine can be calculated by considering the overall efficiency of the wind energy conversion system, including losses in the rotor, generator, and power electronics.

The overall efficiency takes into account various losses, such as mechanical losses in the rotor, electrical losses in the generator, and losses in the power electronics and grid connection.

It's important to note that the power output of a wind turbine is not constant and varies with changes in wind speed and other environmental factors. Wind turbines are designed to operate within a specific range of wind speeds, known as the cut-in and

cut-out wind speeds, to maximize power generation while ensuring safe and efficient operation.

Wind turbine power profile

By defining a power profile, some regions can be defined and establishing operating limits, wind turbine manufacturers ensure safe and reliable operation while maximizing energy production within the turbine's design capabilities.

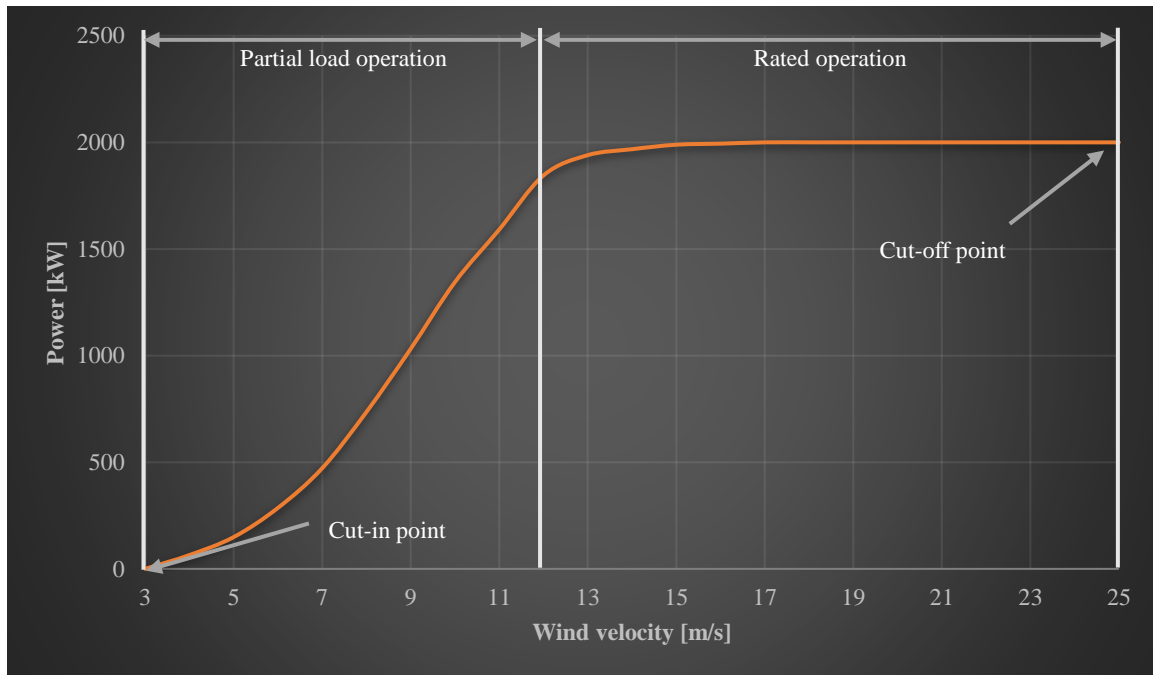


Illustration 29. Typical turbine power curve for a Gamesa G80 model [21].

- **Cut-in point:** This is the minimum wind velocity required for the wind turbine to start producing energy. It is the point at which the wind speed is sufficient to overcome the inertia of the turbine's components and initiate power generation. Common cut-in wind speeds range from 3 to 4 m/s.
- **Partial load operation:** In this region, the wind turbine operates below its nominal conditions. It can be limited by either the wind velocity or the turbine's management system. The turbine produces power, but not at its maximum capacity. The specific wind speeds and power output in this region depend on the design and control strategy of the turbine.
- **Rated operation:** This is the range of wind velocities in which the wind turbine operates at its nominal power output. The turbine's management system, including pitch control, is used to maintain a constant power

production within this range. The rated operation region allows the turbine to generate its maximum power efficiently and reliably.

- **Cut-off point:** This is the maximum wind velocity at which the wind turbine stops producing power. Beyond this wind speed, the turbine's control system triggers a shut-off mechanism, such as activating the brakes, to protect the turbine from excessive loads. The cut-off wind speed is typically set around 25 m/s, but it can vary depending on the turbine design and site-specific conditions.
- **Survival velocity:** This refers to the ultimate wind velocity that a wind turbine can withstand without sustaining permanent damage. Wind speeds exceeding the survival velocity can lead to extreme loads on the turbine components and can cause structural failures. Common survival wind speeds range from 50 to 60 m/s, but again, these values can vary based on turbine design and location.

2.2 Non-Renewable energy sources

2.2.1 Conventional power plants

Conventional power plants, which are often referred to as thermal power plants, utilize fossil fuels such as oil, coal, and gas to generate electricity. There are different methods employed in these plants to convert the energy from fossil fuel combustion into electrical energy.

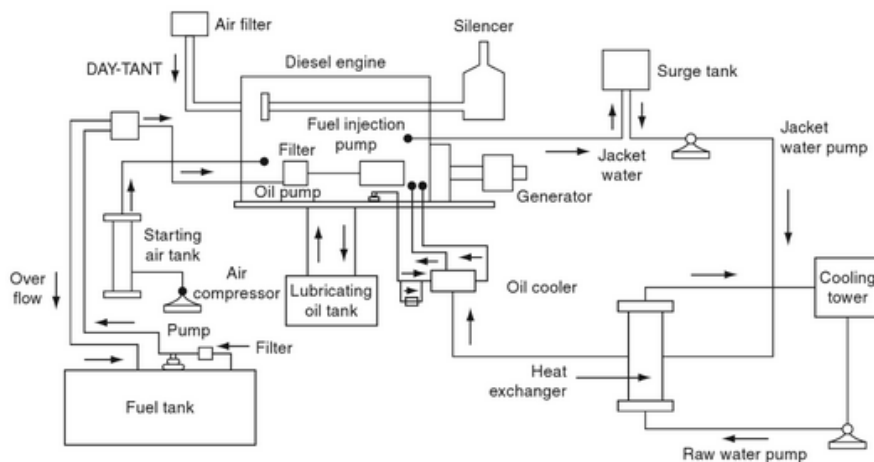


Illustration 30. Scheme for a diesel engine power plant [22].

One method involves the use of diesel combustion engines (see Illustration 30). These engines utilize liquid fuel, such as diesel, which undergoes combustion in a chamber. The energy released from the combustion process is transferred to a piston, which is connected to a crankshaft. The movement of the crankshaft is then used to drive a generator, producing electricity.

Another method involves the use of gas turbines. In this case, the fuel is used to heat a secondary fluid, often water, to produce high-pressure and high-temperature steam or overheated vapor. This steam is then directed to a gas turbine, which is connected to a generator. The high-pressure steam expands in the turbine, causing the turbine blades to rotate. The rotation of the turbine drives the generator to produce electricity.

In both cases, the heat generated by the combustion of fossil fuels is used to produce mechanical energy, which is then converted into electrical energy by the generator. Heat exchangers are utilized to separate the exhaust gases from the combustion process and the thermodynamic fluid, ensuring efficient heat transfer and energy conversion.

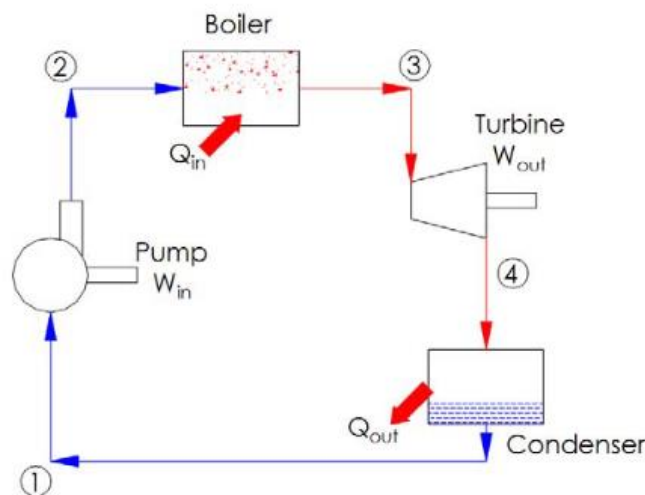


Illustration 31. Scheme simplified of a conventional power plant [23].

A variant of this kind of power plant are the cogeneration power, also known as combined heat and power (CHP) plants, are a variant of conventional power plants that offer increased efficiency by utilizing waste heat generated during the electricity generation process. In these plants, a primary gas cycle, often based on the Brayton cycle, is employed.

The primary gas cycle involves the combustion of fossil fuels, typically natural gas, in a gas turbine. The combustion process drives the turbine, which is connected to a generator to produce electricity. The exhaust gases from the gas turbine, which still contain a significant amount of heat energy, are then directed to a boiler.

In the boiler, the exhaust gases transfer their remaining heat energy to a secondary fluid, usually water, which produces high-pressure steam. This steam can be used for various purposes, such as heating buildings or providing steam for industrial processes. The steam can also be directed to a steam turbine, which is connected to an additional generator to produce more electricity.

By utilizing the waste heat from the primary gas cycle, cogeneration power plants achieve higher overall efficiency compared to traditional power plants. This is because they make use of the heat that would otherwise be wasted in conventional power plants, thereby maximizing the energy output from the fuel source,

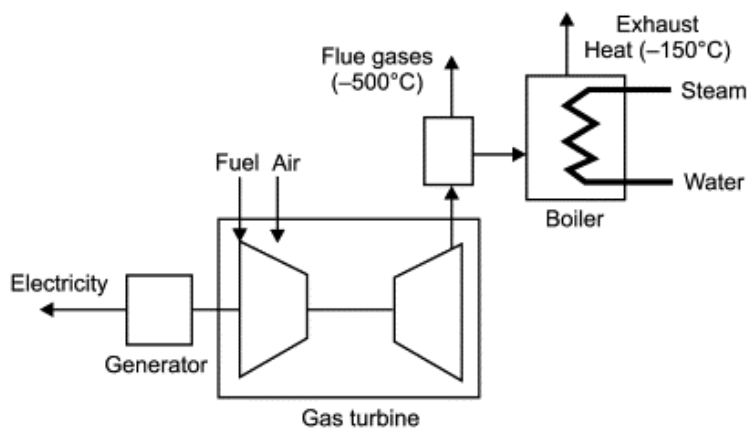


Illustration 32 shows graphically this process.

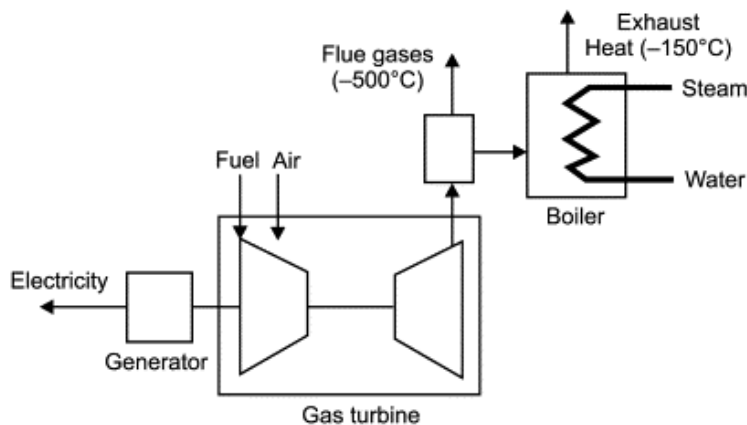


Illustration 32. Scheme simplified of a cogeneration power plant [24].

One of the main drawbacks of these facilities is their environmental impact. The combustion of fossil fuels in conventional and cogeneration power plants releases greenhouse gases, primarily carbon dioxide (CO₂), which contribute to climate change. Meeting environmental regulations and reducing greenhouse gas emissions can be a significant challenge for these power plants.

Additionally, the availability and cost of fuel can pose limitations. Fossil fuels, such as oil, coal, and natural gas, are finite resources and their availability can vary depending on factors like geopolitical tensions, market prices, and extraction costs. Fuel transport and storage logistics also need to be considered, as reliable and efficient supply chains are necessary to ensure the continuous operation of the power plant.

On the other hand, one of the advantages of cogeneration power plants is their ability to quickly respond to changes in electricity demand. These plants can ramp up or down their power generation output relatively faster compared to some other types of power plants. This flexibility allows them to meet sudden increases or decreases in electricity demand and provide a more reliable power supply to the grid.

Furthermore, the waste heat recovery aspect of cogeneration power plants is a significant advantage. By utilizing the waste heat generated during electricity generation, these plants can achieve higher overall efficiency and reduce energy waste. The recovered heat can be used for various applications, such as heating nearby buildings or industrial processes, providing additional benefits in terms of energy conservation and cost savings.

In summary, while cogeneration power plants offer advantages in terms of flexibility and waste heat recovery, they also face challenges related to environmental regulations, fuel availability, and logistical considerations. The overall suitability and sustainability of these plants depend on various factors, including the specific location, energy policies, and advancements in cleaner and more sustainable energy technologies.

2.2.2 Nuclear power

Nuclear power harnesses the energy from atomic reactions, particularly nuclear fission. In the process of nuclear fission, a heavy atomic nucleus, such as uranium-

²³⁵U or plutonium-239, is bombarded with a neutron, causing the nucleus to become unstable and split into two smaller nuclei, along with the release of additional neutrons and a significant amount of heat. This is typically accompanied by the release of gamma radiation.

The splitting of the atomic nucleus releases a large amount of energy due to the conversion of mass into energy, according to Einstein's famous equation, $E = mc^2$, where E represents energy, m represents mass, and c is the speed of light. This energy is in the form of kinetic energy of the fission fragments and the kinetic energy of the released neutrons.

The heat generated from nuclear fission is utilized to produce steam, which drives a turbine connected to a generator, producing electricity. The control of the nuclear fission reaction is crucial to ensure the sustainability and safety of the power plant. This is achieved through the use of control rods, which absorb neutrons and regulate the rate of fission.

It is important to note that nuclear power plants also generate radioactive waste, which needs to be handled and managed properly to prevent environmental contamination and ensure the safety of future generations. The disposal of nuclear waste is a significant challenge associated with nuclear power generation.

Nuclear power has the advantage of producing a large amount of electricity from a relatively small amount of fuel, for example, approximately 24 GWh per kg, in contrast, 1 kg of coal has 8 kWh (3 million times more) [25]. It is a low-carbon energy source and can contribute to reducing greenhouse gas emissions when compared to fossil fuel-based power plants. However, it also poses risks and concerns related to safety, security, and the potential for nuclear accidents, as well as the long-term storage and disposal of radioactive waste.

The use of nuclear power remains a topic of debate, and its future development and deployment will depend on factors such as public opinion, government policies, advancements in reactor technology, and the development of sustainable and safer nuclear fuel cycles [26].

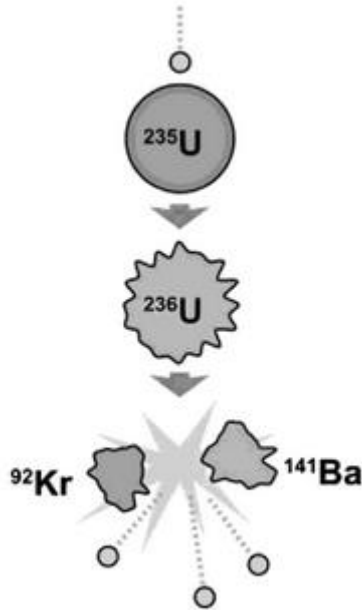
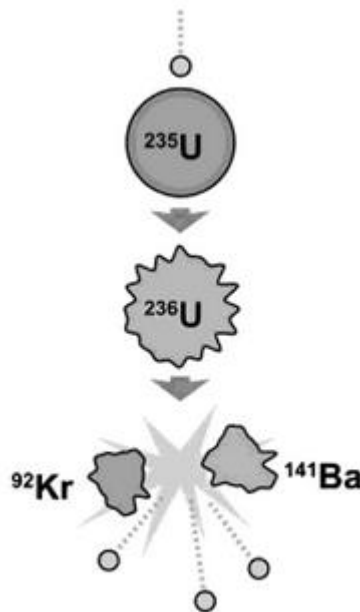


Illustration 33. Fission reaction process.

In a nuclear power plant, the fission reaction occurs when a heavy nucleus, such as uranium-235, absorbs a neutron and becomes unstable. The nucleus then



splits into two smaller nuclei (see

Illustration 33), releasing a large amount of energy in the process. This energy is released as kinetic energy of the fission fragments, as well as the energy carried away by multiple high-energy neutrons. To control the fission reaction and the heat release, several mechanisms are employed.

Control rods are inserted into the reactor core to regulate the fission process. These rods are made of materials, such as the silver-indium-cadmium alloy, that are

effective at absorbing neutrons. By adjusting the position of the control rods within the core, the number of neutrons available to sustain the chain reaction can be controlled. Inserting the control rods deeper into the core increases neutron absorption, slowing down or stopping the fission reaction. Conversely, withdrawing the control rods allows more neutrons to interact with the fuel, increasing the fission rate.

The reactor coolant, which can be heavy water, light water, or a gas, serves multiple purposes. Firstly, it helps to remove heat generated during the fission process from the reactor core. This coolant circulates through the core, absorbing heat and carrying it away to the heat exchanger. By controlling the flow rate and temperature of the coolant, the rate of heat removal can be regulated, thus controlling the temperature of the reactor.

Nuclear power plants have also multiple safety systems in place to ensure safe operation and prevent overheating. These systems include emergency shutdown mechanisms, such as control rod insertion, which can rapidly halt the fission reaction in the event of an emergency. Additionally, passive cooling systems, such as natural circulation or forced convection, ensure that even during power loss, the reactor core can be effectively cooled.

The combination of these control mechanisms allows operators to manage the fission reaction and control the rate of heat release in a nuclear power plant. It ensures that the reactor operates within safe limits and maintains a stable and controlled level of power generation.

2.3 Energetic vector: Hydrogen

2.3.1 Production

Hydrogen production involves generating hydrogen gas, which has various applications in areas such as vehicle fuel, power plants, and chemical manufacturing. There are different methods for producing hydrogen gas, including:

- **Steam Methane Reforming (SMR):** This is the most common method, accounting for approximately 95% [27] of global hydrogen production. It entails reacting natural gas (mainly methane) with steam at high temperatures and pressures to produce hydrogen gas and carbon dioxide. The carbon dioxide is usually captured for storage or other uses.
- **Electrolysis:** This process involves using electrical energy to split water molecules into hydrogen and oxygen gases. It can be powered by renewable energy sources like solar or wind power, making it a potentially sustainable method for hydrogen production.
- **Partial oxidation:** Hydrogen gas can be obtained by reacting a hydrocarbon fuel (such as natural gas, gasoline, or diesel) with oxygen, resulting in hydrogen gas and carbon monoxide¹². The carbon monoxide can then undergo water-gas shift reaction [28] with steam to produce additional hydrogen gas and carbon dioxide.
- **Biomass gasification:** This method involves heating biomass materials like wood chips or agricultural waste in the absence of oxygen, which produces a gas mixture called syngas. Syngas contains hydrogen gas, carbon monoxide, and other gases. The syngas can be separated and purified to obtain hydrogen gas.
- **Thermochemical water splitting:** This approach utilizes heat to break down a metal oxide into oxygen and metal atoms with high efficiency, up to 50% [29]. The metal atoms are then reacted with water to produce hydrogen gas and regenerate the metal oxide, which can be reused in the process. It is a closed-loop system that only consumes water during the process.

¹² Carbon monoxide appears when the amount of oxygen is low.

Hydrogen is not naturally present in its pure form and needs to be extracted from other substances. Once produced, it can be stored and transported for use as an energy source in various applications. Due to its role in energy storage and transfer, hydrogen is often referred to as an energy carrier or vector.

One of the key advantages of hydrogen as an energy carrier is its versatility. It can be utilized in a wide range of applications, including transportation, industrial processes, and power generation. This adaptability makes it an attractive option for meeting diverse energy needs while also potentially reducing greenhouse gas emissions.

Hydrogen can be produced from different feedstocks, such as natural gas, biomass, and renewable energy sources. This flexibility in feedstock selection further enhances its appeal as an energy carrier. Additionally, hydrogen has a high energy density per unit of weight, which means it contains a significant amount of energy relative to its weight. This characteristic makes it a potentially efficient fuel for transportation applications.

When hydrogen is burned, it only produces water and heat, making it a clean and environmentally friendly fuel option. This clean combustion process contributes to the reduction of air pollutants and greenhouse gas emissions.

Considering its versatility, abundance, and clean-burning properties, hydrogen holds promise as an energy carrier for the future. However, there are still challenges associated with large-scale production, storage, and transportation of hydrogen. Ongoing research and development efforts are necessary to overcome these technical and economic barriers and unlock the full potential of hydrogen as an energy carrier diversifying the energy mix in the future [30].

2.3.2 Storage

Hydrogen storage is indeed a critical aspect due to its low density by volume, which presents challenges for certain applications, particularly transportation. Various methods have been developed to address hydrogen storage, including:

- **Compressed gas storage:** Hydrogen can be compressed and stored in high-pressure tanks, typically at pressures ranging from 350 to 700 bar for type IV containers [31]. This method requires tanks that are heavier and

larger than conventional fuel tanks, which may limit their use in certain applications.

- **Liquid hydrogen storage:** Hydrogen can be cooled and stored as a liquid at cryogenic temperatures in specialized tanks [32]. This approach necessitates significant insulation to prevent the hydrogen from evaporating. However, it can be expensive and energy intensive.
- **Chemical hydrogen storage:** Hydrogen can be stored by chemically combining it with other elements, such as metals or organic compounds [32]. This method enables high storage densities but typically requires energy input to release the hydrogen, which can limit its efficiency.
- **Material-based storage:** Certain materials, such as metal hydrides or carbon nanotubes [32], have the ability to absorb or adsorb hydrogen gas. This method offers the potential for high storage densities and is a reversible process. However, it often requires relatively long times and high temperatures or pressures to release the stored hydrogen.

2.3.3 Use

Hydrogen has a wide range of applications in various industries, although its widespread adoption still faces challenges in terms of production, storage, distribution infrastructure, and costs. However, ongoing research and technological advancements are aimed at addressing these challenges and promoting hydrogen as a clean energy source.

Transportation fuel

Hydrogen can be used as a fuel for vehicles, either in hydrogen fuel cell electric vehicles or hydrogen internal combustion engine vehicles. In fuel cell vehicles, hydrogen is used to generate electricity, which powers the vehicle's electric motor. This application produces zero emissions, as the only by-products are water vapor and heat [33].

Industrial processes

Hydrogen is widely used in industrial applications, particularly in petroleum refining, ammonia production, and methanol production. It serves as a reactant or feedstock in various chemical processes and refining operations [34].

Power generation

Hydrogen can be used to generate electricity. It can be directly burned in a turbine or utilized in fuel cells to produce electricity with high efficiencies and lower emissions compared to conventional fossil fuel-based power plants [35].

Energy storage

Hydrogen's high energy density enables large amounts of energy to be stored in tanks for extended periods without degradation. It can be produced from renewable sources during periods of excess generation and later used for power generation or other applications when the supply of renewable energy is limited [36].

Residential and commercial heating

Hydrogen can be burned for space heating or blended with natural gas in existing natural gas infrastructure to provide heating for residential and commercial buildings [37].

Energy and power backup

Hydrogen can serve as a backup power source for critical systems, such as telecommunications, hospitals, and data centres. It offers a reliable and long-duration energy supply during power outages [38].

Hydrogen fuel stations

Hydrogen fuelling stations are being established to support the growing number of hydrogen-powered vehicles. These stations provide the necessary infrastructure for refuelling fuel cell electric vehicles, enabling longer-range travel, and promoting the adoption of hydrogen-powered transportation.

In fact, regarding to the diverse range of applications highlights the versatility and potential of hydrogen as an energy carrier. Continued advancements in hydrogen technologies and infrastructure will play a crucial role in realizing its full potential as a clean and sustainable energy source.

2.3.4 Scalability

The scalability of hydrogen production and utilization is a crucial aspect for its widespread adoption as an energy carrier. Here are the key points regarding the scalability of hydrogen.

Regarding to the production scalability, it can be obtained at various scales, ranging from small-scale systems for localized applications to large-scale industrial facilities [27]. Expanding production capacity, diversifying production sources (such as electrolysis from renewable methods) and optimizing production processes are essential for achieving greater scalability.

Developing a robust hydrogen distribution and storage network is necessary to support the widespread use of hydrogen. Additionally, establishing hydrogen refuelling stations for transportation applications is crucial. Scaling up infrastructure requires significant investment and coordination among stakeholders, including governments, industries, and energy producers.

Achieving scalability often involves cost reductions through economies of scale, technological advancements, and increased production volumes. Currently, hydrogen production from fossil fuels is more cost-effective compared to renewable energy-powered electrolysis. However, the declining costs of renewable energy and ongoing research and development efforts are improving the cost competitiveness of renewable hydrogen [27].

Supportive policies, regulations, and market mechanisms play a significant role in promoting the scalability of hydrogen. Governments and industry stakeholders are implementing strategies and incentives to foster the growth of hydrogen infrastructure [39], attract investment, and stimulate demand for hydrogen-based products.

Collaboration among countries can facilitate knowledge sharing, technology transfer, standard harmonization, and the establishment of global supply chains for hydrogen. International partnerships and agreements can help accelerate the deployment of hydrogen infrastructure and foster its scalability on a global scale, aligning with climate goals and reducing dependence on non-renewable sources.

While there are challenges to overcome, such as technological advancements, infrastructure development, and cost reduction, the scalability of hydrogen is feasible. Concerted efforts from industry, governments, and research institutions are needed to

drive the scalability of hydrogen and realize its potential as a clean and sustainable energy carrier.

2.4 Environmental European policies

The European Union (EU) has implemented various environmental policies to address climate change, protect the environment, and promote sustainable development. Here are the key points regarding EU environmental policies [40]:

- **Greenhouse gas emissions reduction:** The EU aims to reduce greenhouse gas emissions by at least 55% by 2030 compared to 1990 levels, with the ultimate goal of achieving near climate neutrality (80 – 95%) by 2050 [41]. This is supported by initiatives such as the EU Emissions Trading System (ETS) and the Effort Sharing Regulation, which set emission reduction targets for different sectors.
- **Biodiversity protection:** The EU has adopted a comprehensive biodiversity strategy for 2030, which focuses on protecting and restoring biodiversity and ecosystems. Measures include the establishment of the Natura 2000 network of protected areas and the EU Timber Regulation to combat illegal logging [42].
- **Circular economy:** The EU promotes a circular economy where resources are used more efficiently, and waste is minimized. This involves setting waste reduction and recycling targets, implementing product design rules, and introducing eco-labelling schemes [43].
- **Air quality:** The EU addresses air pollution in cities by establishing standards to protect human health and the environment. Measures are implemented to reduce air pollution from various sources, including industry, transport, and agriculture.
- **Water quality:** Recognizing the importance of water as a valuable resource, the EU has established a legal framework to ensure that all bodies of water within the EU achieve good ecological status by 2027 [44]. This aims to protect and improve water quality.

These environmental policies are designed to promote sustainable development and ensure the protection of the environment for future generations. Through these

measures, the EU aims to mitigate climate change, preserve biodiversity, promote resource efficiency, improve air quality, and safeguard water resources.

3 Dynamic Virtual Power Plant (DVPP)

3.1 Definition

A Dynamic Virtual Power Plant (DVPP) is a system that integrates multiple distributed energy resources, such as solar plants, windmills, energy storage systems, and connected devices, into a coordinated and virtual power plant. Unlike traditional centralized power plants, a DVPP utilizes smaller-scale resources to create a flexible and responsive energy network-[45].

The operation of a DVPP relies on advanced software and communication technologies. It optimizes the energy generation, consumption, and storage capabilities of the integrated resources by coordinating their operation. This allows the DVPP to mimic the behaviour of a conventional power plant, delivering reliable and dispatchable power to the grid.

One notable feature of a DVPP is its ability to dynamically adjust the output of each resource in real-time. It can respond to changes in electricity demand, market prices, and grid conditions, ensuring the overall efficiency and operation of the virtual power plant [45]. For instance, during periods of high demand or grid instability, the DVPP can rapidly increase the output of each energy producer to provide additional power and support to the grid.

Furthermore, a DVPP enables the participation of each energy producer in various energy markets, such as wholesale electricity markets, ancillary services markets, and demand response programs. By aggregating the capabilities of multiple distributed resources, the DVPP can offer services such as energy trading, frequency regulation, peak shaving, and load balancing [45]. This not only generates revenues for the owners but also contributes to grid stability.

The benefits of implementing a DVPP are numerous. It enhances grid flexibility and stability by integrating diverse energy resources and supporting the integration of intermittent renewables. It optimizes costs by evaluating each element of the grid based on electricity prices and maximizing revenue for each owner [45]. It improves energy efficiency by optimizing the operation of producers and enabling demand response capabilities. Additionally, it promotes decentralization and resilience,

allowing other producers to compensate for any deficits and ensuring continuous power supply during disruptions.

Overall, a DVPP represents an innovative approach to managing energy distribution in interconnected grids. By leveraging distributed energy resources and advanced control systems, it creates a more flexible, efficient, reliable, and sustainable power grid.

3.2 Ancillary services: Frequency and voltage

Frequency and voltage control are critical for maintaining grid stability and reliability. Traditionally, these services have been provided by large-centralized power plants due to their high-power control capabilities. However, with the integration of renewable energy sources and distributed energy resources, the role of ancillary services is evolving.

In the context of a Dynamic Virtual Power Plant (DVPP), the challenge lies in coordinating and aggregating the capabilities of multiple distributed resources to provide frequency and voltage control. This requires advanced control systems and communication technologies to manage the diverse resources within the DVPP [46].

For frequency control, energy storage systems within a DVPP can respond quickly to deviations in grid frequency. They can inject or absorb power into the grid to help stabilize the frequency [47]. By actively managing the power output of energy storage systems, the DVPP can support grid frequency regulation.

Similarly, voltage control within a DVPP can be achieved by adjusting the reactive power output of each resource. By coordinating the reactive power capabilities of distributed resources, the DVPP can help maintain grid voltage within acceptable limits.

The advantage of a DVPP in providing ancillary services is its ability to leverage the flexibility and responsiveness of individual resources. Through advanced control systems, the DVPP can optimize the response of each resource to changes in grid conditions. This allows for more efficient and cost-effective provision of ancillary services compared to relying solely on centralized power plants.

As the penetration of renewable energy sources increases, DVPPs have the potential to play a significant role in providing ancillary services. Their ability to integrate and coordinate diverse distributed resources enables them to contribute to grid stability and accommodate the variability of renewable energy generation in modern power systems.

3.2.1 Frequency control

Frequency control is crucial in maintaining the overall stability of the grid by balancing electricity generation and consumption. Ancillary services, such as load-frequency control (LFC) and primary and secondary frequency response, play a vital role in ensuring that the frequency remains within the acceptable range.

Load-frequency control (LFC), also known as Automatic Generation Control (AGC), continuously adjusts the generation output to match the electricity demand in real-time. It monitors the grid's frequency and communicates with power plants to make necessary adjustments. If the frequency is too high, generation is reduced, and if the frequency is too low, generation is increased. This helps maintain the frequency within the normal range [46] [48].

Primary frequency response is provided by conventional power plants with inherent inertia. The rotational inertia of these generators helps slow down the frequency decline when there is a sudden increase in demand or loss of generation. Similarly, when there is an excess of generation, the rotational inertia assists in slowing down the frequency rise [49].

Secondary frequency response provides additional support to primary frequency control. It involves the active participation of fast-acting reserves, energy storage systems (ESS), and demand response. These resources can quickly inject or absorb power to help stabilize the frequency during sudden disturbances. For example, if the frequency drops, ESS or demand response programs can inject power into the grid to support frequency recovery [49].

The increasing integration of renewable energy sources poses challenges for frequency control due to their variable and unpredictable nature. However, it also presents opportunities. Renewable resources, such as solar power, can participate in

frequency control markets by dynamically adjusting their power output based on frequency deviations. This can be achieved through smart inverters, allowing renewable energy sources to contribute to frequency control and grid stability.

Overall, frequency control measures are crucial in maintaining grid stability by ensuring the balance between electricity generation and consumption. The integration of advanced control technologies and the participation of various resources, including conventional power plants, energy storage systems, and renewable energy sources, can help optimize frequency control and enhance the reliability and resilience of the grid.

3.2.2 Voltage control

Voltage control is essential for maintaining stable and acceptable voltage levels throughout the grid. Fluctuations in voltage can have negative effects on electrical equipment and appliances, so it is crucial to regulate and control voltage within specified limits [50]. Within a Dynamic Virtual Power Plant (DVPP), voltage control can be achieved by coordinating the operation of distributed energy resources. There are several methods and devices used for voltage control.

Voltage regulators and transformers are commonly used to adjust voltage levels at various points in the grid [50]. Voltage regulators can modify the transformer tap settings to increase or decrease the voltage as needed, while transformers can step up or step down the voltage.

Reactive power is a component of AC signals that can be controlled to modify voltage levels. Reactive devices such as capacitors and reactors (inductors) are employed to inject or absorb reactive power at specific locations in the grid, helping regulate voltage levels [51]. Capacitors can supply leading reactive power, while reactors can absorb lagging reactive power.

Power factor is the ratio between active power (real power) and apparent power in an AC system. Inverter-based devices, such as those used in renewable energy systems, can adjust their output power factor to a desired level, typically close to unity [52]. This helps improve the power factor and overall voltage stability in the grid.

By coordinating the operation of distributed energy resources within a DVPP, including adjusting reactive power outputs and optimizing power factor, voltage control

can be effectively managed. Advanced control algorithms and communication technologies enable the DVPP to respond to voltage disturbances and maintain voltage levels within acceptable ranges, ensuring the stability and reliable operation of the grid.

4 Geographic delimitation

When delimiting a geographic region to develop a Dynamic Virtual Power Plant (DVPP), several factors need to be considered. In the case of Andalusia and Valencia, the selection of the region is based on the availability of reliable and updated information from local organizations regarding the physical structure, regulatory boundaries, grid network structure, resource availability, and market considerations.

The delimitation of the region for a DVPP involves both strategic and technical considerations. Some general technical factors that are taken into account include power line losses, harmonic deviations, reactive power injected into the grid, and temperature effects on material properties. These factors impact the overall operation and performance of the DVPP. However, for the simplification of the analysis, the simulation of the physical layer is out of the scope of this analysis

In the case of the selected regions the choice of renewable energy resources is based on the actual potential resources available in the region. Three types of renewable energy sources have been chosen: photovoltaic solar energy, onshore wind power, and offshore wind power. Data of the potential resources for these energy sources can be gathered from websites such as NASA, renewables.ninja, and PVGIS. This data helps in evaluating the feasibility and potential of incorporating these renewable energy sources into the DVPP.

By considering the specific characteristics and potential resources of a chosen geographic region, a DVPP can be developed and optimized to leverage the available renewable energy sources and effectively contribute to the stability, reliability, and sustainability of the local power grid.

For the ease of calculation and we have grouped the plants by province.

Considering we have considered the following locations for the calculation

N°	Source	Autonomous Community	Location	Coordinates
1A	Photovoltaic	Andalusia	Huelva	37.2169, -6.8037
2A			Sevilla	37.0891, -5.9941
3A			Cádiz	36.367, -6.0981
4A			Málaga	36.6710, -4.6942
5A			Granada	37.0952, -3.7841
6A			Almería	37.0950, -2.2360
1V		Valencia	Valencia	39.5317, -1,3198
2V			Castello	39.8498, -0.1296
3V			Alicante	38.2452, -0.6997
1A	Onshore wind power	Andalusia	Huelva	37.2255, -7.102661
2A			Sevilla	37.438775, -6.1337
3A			Cádiz	36.2533, -5.7043
4A			Córdoba	38.2081, -4.91418
5A			Granada	37.046957, -3.380562
6A			Almería	36.8469, -2.2373
1V		Valencia	Valencia	39.2145, -0.8616
2V			Castello	40.4701, -0.0639
3V			Alicante	38.6490, -0.2562
1A	Offshore wind power	Andalusia	Almería	36.6287, -2.1835
1V		Valencia	Alicante	38.748, 0.3537

Table 4. Location of the selected places for new power plants in Andalusia.

4.1 Demand

In order to define a base of analysis for the optimization model, it is essential to gather accurate demand data. This crucial information is obtained from the Red Eléctrica de España, which provides comprehensive and reliable data on energy demand and generation. Data required includes an annual record for each hour in a single day. For the purpose of this simulation, the starting year for the analysis is set as 2022, ensuring that the model is based on recent and relevant data. By using this dataset, the optimization model can evaluate and address the energy needs in the regions of Andalusia and Valencia, enabling the identification of optimal solutions for the energy system.

On the REE website we have demand data for the entire peninsula every 5 minutes. This generates a typical hourly demand curve and with this data we can construct an average consumption distribution curve for 24 hours, with this and

extrapolating to the monthly demand data for the autonomous communities we can construct an approximate hourly demand distribution curve for the whole year. This curve is shown in the following illustration:

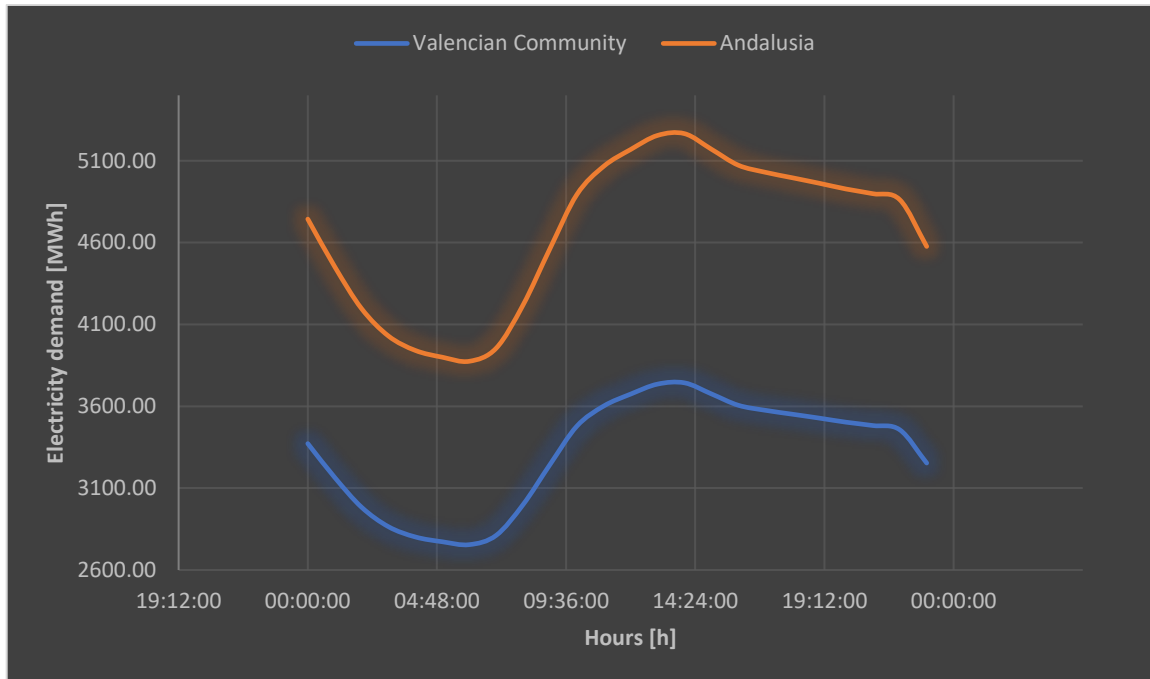


Illustration 34. Typical-day demand profile per hour. Data is courtesy of REE.

Illustration 34 indicates the usual behaviour of electricity demand in the autonomous communities of Andalusia y Valencia, notice that the electricity consumption in Andalusia is higher than Valencian Community. Both regions show a similar pattern observed in several regions. Typically, the electricity exhibits a peak during the daytime hours, particularly in the morning and early evening when commercial and residential activities are at their highest. This is attributed to the use of appliances, lighting, and other electrical devices during these periods.

During the daytime, when businesses are operational, there is usually an increased demand for electricity due to industrial activities, office operations, and commercial establishments. As the evening approaches, residential electricity consumption tends to rise as people return home, leading to a further increase in demand.

Conversely, during the nighttime hours, electricity demand generally decreases as commercial activities wind down and households reduce their energy usage. This period often corresponds to the lowest demand levels during a 24-hour cycle.

It is important to note that the specific demand patterns may vary based on factors such as seasonality, weather conditions, and local characteristics of the Valencia and Andalusia. Local industries, tourism, and other regional factors can influence the overall demand profile as well. Detailed data and analysis from regional energy authorities can provide a more accurate and specific understanding of the daily electricity demand behaviour in these regions.

4.2 Installed capacity

The following tables show the distribution of the installed capacity for each region in this document

N°	Source	Installed capacity [MW]
1	Cogeneration	2854
2	Combined cycle	441
3	Hydropower	642
4	Pumped Storage Hydropower	1512
5	Photovoltaic	423
6	Renewable waste	63
7	Solar thermal	50
8	Wind power	1243
9	Other renewables	13
10	Nuclear	1064

Table 5. Installed capacity in Valencia for 2022. Data courtesy by REE.

N°	Source	Installed capacity [MW]
1	Cogeneration	704
2	Combined cycle	5952
3	Coal	570
4	Hydropower	623
5	Pumped storage hydropower	585
6	Photovoltaic	4208
7	Renewable waste	51
8	Solar thermal	1000
9	Wind power	3613
10	Other Renewables	451

Table 6. Installed capacity in Andalusia for 2022. Data courtesy by REE.

To simplify our analysis cases, we have not considered solar thermal generation or combined installed capacities of less than 300MW.

5 Methodology

5.1 Optimization method: Levelized Cost of Energy

The methodology for evaluating and optimizing the Dynamic Virtual Power Plant (DVPP) in the selected regions involves using the Levelized Cost of Energy (LCOE) as the optimization method. The LCOE is a metric that enables the comparison of different energy generation scenarios and helps in selecting the most suitable option for the overall model.

The LCOE represents the average present cost per unit of electricity produced over the lifetime of the project. It takes into account various cost factors such as development, construction, operation, maintenance, and fuel costs¹³. By considering these costs, the LCOE provides a comprehensive view of the economic feasibility of different energy generation sources.

To calculate the LCOE, the present value of money is used, which takes into account the time value of money. The discount rate is applied to represent the costs and benefits from the future in present terms. The discount rate reflects the rate of return or interest rate expected from the project. Typical values for energy projects can range from 3% to 10% for plant design of 20 years, and it can depend on various factors [53].

By utilizing the LCOE and applying the appropriate discount rate, different energy generation scenarios, including photovoltaic solar energy, onshore wind power, and offshore wind power, can be evaluated and compared. This analysis helps in determining the most cost-effective and efficient combination of energy resources for the DVPP.

It is important to note that in addition to the LCOE, other factors such as grid integration, environmental impact, and regulatory requirements should also be considered in the overall evaluation and optimization process. The LCOE serves as a

¹³ For renewable sources like PV and wind power, fuel is available in nature and free to use it.

valuable metric for economic assessment, but it should be used in conjunction with other relevant criteria to make informed decisions regarding the DVPP implementation.

$$LCOE = \frac{CAPEX + \frac{OPEX + RC + FC}{(1+i)^t}}{\frac{E_t}{(1+i)^t}} \quad \text{Eq. 15}$$

In the Levelized Cost of Energy (LCOE) calculation, the capital or initial expenditures (CAPEX), operative expenditures (OPEX), replacement costs (RC), and fuel costs (FC) are taken into account to evaluate the overall cost of generating electricity. These costs are considered for each year of the project's lifespan and are converted to present value using the discount rate.

The CAPEX represents the upfront capital costs associated with the installation of the energy generation system. It includes expenses such as equipment purchase, construction, and installation.

The OPEX refers to the operational expenditures incurred after the installation, including costs related to maintenance, repairs, and general operation of the energy generation system.

The RC represents the costs of replacing certain components or equipment during the project's lifespan. If the lifespan of the project is the same for all installations being compared, the RC can be neglected since it will be the same for each scenario.

The FC represents the fuel costs, if applicable, associated with the energy generation system. This is relevant for scenarios that involve fuel-based generation technologies such as fossil fuel power plants.

To calculate the LCOE, the energy produced each year (E_t) is multiplied by the corresponding costs (CAPEX, OPEX, and FC) for that year. These costs are then converted to present value using the discount rate (i). The present value costs for each year are summed up, and the total is divided by the cumulative energy produced over

the project's lifetime to obtain the levelized cost per kilowatt-hour (kWh) of electricity generated.

By using Euros as the currency unit and kWh as the energy unit, the LCOE is expressed as Euros per kilowatt-hour (€/kWh), providing a standardized measure to compare different energy generation scenarios and make informed decisions regarding the most cost-effective option.

It is worth noting that the specific cost components and their values will depend on the project, technology, market conditions, and other factors. Conducting a thorough analysis and considering the relevant costs for each scenario will ensure accurate LCOE calculations and effective decision-making.

5.2 System modelling

5.2.1 Elements included and constraints included in the model

Nuclear power

In the system modelling, the inclusion of nuclear power is considered as a baseline energy source, assuming that the nuclear power plants will operate at their nominal output capacity throughout the modelled period. This means that the nuclear production mathematical model assumes a constant production level from nuclear power. The constraints related to nuclear power can include the following:

- **Power Capacity** $P_{Nu[t][i]}$: The power capacity of existing nuclear power plants is considered as the maximum output that can be generated by these facilities. It is assumed that the available nuclear power capacity is sufficient to meet the energy demand of the grid, and there is no need to incorporate new nuclear facilities.
- **Constant Production** $(x_{Nu})_{[t][i]}$: The mathematical model for nuclear production assumes a constant generation level, meaning that the nuclear power plants will operate consistently at their nominal output capacity without significant fluctuations. This assumption simplifies the modelling process by assuming a steady and reliable source of electricity from nuclear power.

$$(x_{Nu})_{[t][i]} = P_{Nu[t][i]} \forall i, \forall t \quad \text{Eq. 16}$$

It is important to note that the specific details and constraints of the nuclear power modelling may vary depending on the specific characteristics and operational parameters of the nuclear power plants in the modelled region. Additionally, the model should also consider any regulatory constraints, safety considerations, and other factors that are relevant to the operation of nuclear power plants in the given context.

Hydropower

In the system modelling, for hydropower facilities that are not equipped with pumping capabilities and rely on natural recharge, the following considerations are taken into account:

- **Instant Power Supplied** $(x_{HP})_{[t][i]}$: The instant power supplied by each hydropower facility i during a specific time interval t is represented by x_{HP} . This parameter indicates the power output of the hydropower facility at a given moment.
- **Installed Capacity** $P_{HP[t][i]}$: The maximum power generated by a hydropower facility must be less than or equal to its installed capacity. This constraint ensures that the power generation does not exceed the maximum capacity of the facility.
- **Maximum Difference Power Production** $|(x_{HP})_{[t+1][i]} - (x_{HP})_{[t][i]}|$: The model includes a constraint that limits the maximum difference in power production between two consecutive intervals. This constraint ensures that the power generation does not fluctuate significantly between intervals.

$$(x_{HP})_{[t][i]} \leq P_{HP[t][i]} \forall i, \forall t \quad \text{Eq. 17}$$

$$|(x_{HP})_{[t+1][i]} - (x_{HP})_{[t][i]}| \leq \Delta P_{HP[i]} \forall i, \forall t \quad \text{Eq. 18}$$

The maximum difference power production allowed between intervals is determined by the capacity variation given for the same interval. This means that the power generation can vary within a specific range, taking into account the capacity variation constraints.

It is important to note that the specific values and constraints for each hydropower facility may vary depending on its characteristics, such as installed

capacity, natural recharge rate, and operational parameters. The model should consider these factors to accurately represent the behaviour of hydropower facilities in the given system.

Pumped storage hydropower

In the system modelling, the pumped storage hydropower plants are considered, which have the capability to both generate power and absorb excess power from the grid by utilizing a pumping system. The model takes into account two working schemes: grid injection (reservoir discharge) and grid absorption (reservoir charge). The constraints for these schemes are as follows:

- **Power Generation (Grid Injection):** The instant power generated by each pumped storage hydropower facility i during a specific time interval t is represented by $[(x_{HP})_{Dis}]_{[t][i]}$. This parameter indicates the power output of the facility when it is discharging stored energy back into the grid.
- **Power Absorption (Grid Charging):** The instant power absorbed by each pumped storage hydropower facility i during a specific time interval t is represented by $[(x_{HP})_{Char}]_{[t][i]} \leq P_{P[t][i]}$. This parameter indicates the power intake of the facility when it is charging the reservoir by absorbing excess power from the grid.
- **Installed Power:** The installed power capacity for turbines, represented by P_T , may not be the same as the installed power capacity for the pumping system, represented by P_P . This accounts for the possibility of having different power capacities for the generation and pumping components of the pumped storage hydropower plant.
- **Maximum Power Production Difference:** Similar to other types of hydropower facilities, there is a constraint on the maximum difference in power production between consecutive time intervals for both grid injection and grid absorption conditions. This constraint ensures that the power generation or absorption does not exhibit significant fluctuations between intervals.

$$[(x_{HP})_{Dis}]_{[t][i]} \leq P_{T[t][i]} \quad \forall i, \forall t \quad \text{Eq. 19}$$

$$[(x_{HP})_{Char}]_{[t][i]} \leq P_{P[t][i]} \quad \forall i, \forall t \quad \text{Eq. 20}$$

$$|[(x_{HP})_{Dis}]_{[t+1][i]} - [(x_{HP})_{Dis}]_{[t][i]}| \leq \Delta P_{T[i]} \quad \forall i, \forall t \quad \text{Eq. 21}$$

$$|[(x_{HP})_{Char}]_{[t+1][i]} - [(x_{HP})_{Char}]_{[t][i]}| \leq \Delta P_{P[i]} \quad \forall i, \forall t \quad \text{Eq. 22}$$

The specific values and constraints for each pumped storage hydropower facility, including the installed power capacities and power production/absorption limits, would depend on the characteristics and operational parameters of each individual facility. These parameters should be considered in the model to accurately represent the behaviour of pumped storage hydropower plants in the system.

An energy balance can be performed in order to determine the amount of energy is already stored in the dams.

$$E_{Res} = E_{Res[t-1][i]} + E_{Char[t][i]} - E_{Dis[t][i]} \quad \forall i, \forall t \quad \text{Eq. 23}$$

In the model, the energy balance for a hydropower facility takes into account the previous instant condition. However, it is important to note that depending on the infrastructure of the hydropower facility, some facilities may have the capability to work in both charge and discharge modes simultaneously.

For the purpose of simplification and modelling efficiency, the current approach considers only one of the scenarios at a time, either charge or discharge, but not both simultaneously. This simplification allows for a more straightforward representation of the energy balance within the model.

By focusing on one scenario at a time, the model can accurately capture the behaviour and constraints associated with either charging the reservoir by absorbing excess power from the grid or discharging stored energy back into the grid. This simplification helps to streamline the modelling process and ensure that the energy balance calculations are performed effectively.

Photovoltaic and wind power (onshore and offshore)

In the model, the photovoltaic (PV) and wind power plants are assumed to directly generate electricity and supply it to the grid without the presence of intermediate energy storage systems like batteries, supercapacitors, or flywheels. Therefore, the production of these renewable energy sources is directly linked to the availability of the solar irradiation for PV and wind speed for wind power at any given

moment. The power generation from PV and wind sources is subject to certain constraints and limitations.

For PV power generation, the instantaneous power output is represented by x_{PV} for a specific time t and for each PV plant i . Similarly, for wind power generation, the instantaneous power output is represented by x_{WP} for a specific time t and for each wind power plant i .

$$(x_{PV})_{[t][i]} \leq P_{PV[t][i]} \quad \forall i, \forall t \quad \text{Eq. 24}$$

$$(x_{WP})_{[t][i]} \leq P_{WP[t][i]} \quad \forall i, \forall t \quad \text{Eq. 25}$$

To ensure a smooth and reliable operation, there are constraints on the maximum production allowed between intervals. The maximum difference in power production between consecutive intervals must not exceed the capacity variation given for the same interval. This constraint helps maintain stability and accounts for the inherent variability and intermittency of solar and wind resources.

$$|(x_{PV})_{[t+1][i]} - (x_{PV})_{[t][i]}| \leq \Delta P_{PV[i]} \quad \forall i, \forall t \quad \text{Eq. 26}$$

$$|(x_{WP})_{[t+1][i]} - (x_{WP})_{[t][i]}| \leq \Delta P_{WP[i]} \quad \forall i, \forall t \quad \text{Eq. 27}$$

By considering these constraints, the model accurately represents the power generation capabilities and limitations of PV and wind power plants. It allows for a realistic representation of the variability and unpredictability of these renewable energy sources while ensuring that the power generation remains within acceptable limits.

Hydrogen production and consumption

In the case of hydrogen facilities, their behaviour in the model is simplified and treated similarly to a battery system.

The instantaneous power delivered by the hydrogen facilities is defined as the power provided or absorbed from the grid. This value is always less than the maximum power capacity of the electrolyser (for hydrogen production) and the hydrogen fuel cell (for electricity production).

$$\left[(x_{Hy})_{Ab} \right]_{[t][i]} \leq P_{El[t][i]} \quad \forall i, \forall t \quad \text{Eq. 28}$$

$$\left[(x_{Hy})_{Gen} \right]_{[t][i]} \leq P_{HFC[t][i]} \quad \forall i, \forall t \quad \text{Eq. 29}$$

Similar to other cases, there is a constraint on the maximum power production difference between time intervals for each condition. This constraint ensures that the power production or consumption by the hydrogen facilities does not exceed the specified capacity variation for a given time interval.

$$\left| \left[(x_{Hy})_{Ab} \right]_{[t+1][i]} - \left[(x_{Hy})_{Ab} \right]_{[t][i]} \right| \leq \Delta P_{El[i]} \quad \forall i, \forall t \quad \text{Eq. 30}$$

$$\left| \left[(x_{Hy})_{Gen} \right]_{[t+1][i]} - \left[(x_{Hy})_{Gen} \right]_{[t][i]} \right| \leq \Delta P_{HFC[i]} \quad \forall i, \forall t \quad \text{Eq. 31}$$

At this point, it is necessary to evaluate the amount of energy stored in tanks, for this reason, an energy balance must be performed to quantify the net energy stored.

$$E_{Tank} = E_{Tank[t-1][i]} + E_{Ab[t][i]} - E_{Gen[t][i]} \quad \forall i, \forall t \quad \text{Eq. 32}$$

Note that for performing the energy balance, the previous instant condition is needed, and depending on the facility infrastructure, some of them are allowed to work in charge and discharge simultaneously. For the development of the model, it is just considered one of both scenarios (charging or discharging but not both at the same time).

$$(E_{Tank})_{min} \leq E_{Tank} \leq (E_{Tank})_{max} \quad \text{Eq. 33}$$

$$(x_{Hy})_{Gen} = \frac{E_{Gen}}{t} \quad \text{Eq. 34}$$

$$(x_{Hy})_{Ab} = \frac{E_{Ab}}{t} \quad \text{Eq. 35}$$

Eq. 33 represents the state of charge of the tank, which indicates how much energy is stored at a given time. This is limited to the maximum amount of energy that can be stored in all the tanks considered in the system.

Eq. 34 and Eq. 35 define the relationship between energy and power. In the context of the model, the time interval for evaluation is set to 1 hour, which means that the power and energy values are considered equivalent within this time interval. This simplification allows for a tractable model and ensures that the energy balance is properly accounted for within each hourly time step. However, it is essential to keep in

mind that this simplification might not fully capture the dynamic behaviour of the system in shorter timeframes.

In summary, Eq. 33 ensures that the energy stored in the tank does not exceed its maximum capacity, while Eq. 34 and Eq. 35 relate the energy and power values for an hourly time step, enabling the model to perform energy balancing calculations effectively.

By considering these constraints and modelling the hydrogen facilities in a manner similar to battery systems, the model can effectively represent the behaviour of the hydrogen facilities in the overall energy system optimization.

Energy balance

In the model, the energy balance is performed for each time gap individually, taking into account the energy demand, generation, and absorption within the system. This allows for a comprehensive evaluation of the energy flows and ensures that the contributions of each element in the system are appropriately adjusted to meet the varying demand.

The energy balance takes into consideration the total energy demanded by the grid during a specific time gap and compares it to the total energy generated by all the power sources, including nuclear, hydropower, photovoltaic, and wind power plants. Additionally, it considers the energy absorbed or stored in cases where hydrogen production or battery charging is part of the system.

By performing this energy balance for each time gap, the model can accurately assess the adequacy of the energy supply and determine if any adjustments or additional measures are necessary to meet the demand. It provides a dynamic representation of the energy exchange within the system and ensures that the system operates efficiently and reliably.

$$G_{e[t]} = D_{[t]} + \sum_{i=1}^n [(x_{HP})_{char}]_{[t][i]} + \sum_{i=1}^n [(x_B)_{char}]_{[t][i]} + \sum_{i=1}^n [(x_{Hy})_{Ab}]_{[t][i]} \quad \forall i, \forall t$$

Eq. 36

$$\begin{aligned}
G_{e[t]} = & \sum_{i=1}^n (x_{Nu})_{[t][i]} + \sum_{i=1}^n (x_{HP})_{[t][i]} + \sum_{i=1}^n [(x_{HP})_{Dis}]_{[t][i]} + \sum_{i=1}^n (x_{PV})_{[t][i]} \\
& + \sum_{i=1}^n (x_{WP})_{[t][i]} + \sum_{i=1}^n [(x_B)_{Dis}]_{[t][i]} + \sum_{i=1}^n [(x_{Hy})_{Gen}]_{[t][i]}
\end{aligned}
\tag{Eq. 37}$$

Cost definition

For each technology, the costs in the model are represented as a combination of capital expenditures (CAPEX) and operational and maintenance expenses (OPEX). These cost components help in evaluating the overall economic viability and sustainability of the system.

These cost components, along with the energy production and operational characteristics of each technology, are used in the model to evaluate the levelized cost of energy (LCOE) and compare different scenarios to determine the most economically viable options for the system.

$$\begin{aligned}
CAPEX_{Ren} = & \sum_{i=1}^n P_{HP[i]} \cdot CAPEX_{HP} + \sum_{i=1}^n P_{T[i]} \cdot CAPEX_T \\
& + \sum_{i=1}^n P_P[i] \cdot CAPEX_P + \sum_{i=1}^n P_{PV[i]} \cdot CAPEX_{PV} \\
& + \sum_{i=1}^n P_{WP[i]} \cdot CAPEX_{WP} + \sum_{i=1}^n P_B[i] \cdot CAPEX_B \\
& + \sum_{i=1}^n P_{El[i]} \cdot CAPEX_{El} + \sum_{i=1}^n P_{HFC[i]} \cdot CAPEX_{HFC}
\end{aligned}
\tag{Eq. 38}$$

$$CAPEX_{Non-Ren} = \sum_{i=1}^n P_{Nu[i]} \cdot CAPEX_{Nu}
\tag{Eq. 39}$$

$$\begin{aligned}
OPEX_{Ren} = & \sum_{t=1}^t \sum_{i=1}^n (x_{HP})_{[t][i]} \cdot OPEX_{HP} + \sum_{t=1}^t \sum_{i=1}^n [(x_{HP})_{Dis}]_{[t][i]} \cdot OPEX_T \\
& + \sum_{t=1}^t \sum_{i=1}^n [(x_{HP})_{Char}]_{[t][i]} \cdot OPEX_P + \sum_{t=1}^t \sum_{i=1}^n (x_{PV})_{[t][i]} \\
& \cdot OPEX_{PV} + \sum_{t=1}^t \sum_{i=1}^n (x_{WP})_{[t][i]} \cdot OPEX_{WP} \\
& + \sum_{t=1}^t \sum_{i=1}^n [(x_B)_{Dis}]_{[t][i]} \cdot (OPEX_B)_{Dis} \\
& + \sum_{t=1}^t \sum_{i=1}^n [(x_B)_{Char}]_{[t][i]} \cdot (OPEX_B)_{Char} \\
& + \sum_{t=1}^t \sum_{i=1}^n [(x_{Hy})_{Ab}]_{[t][i]} \cdot OPEX_{El} \\
& + \sum_{t=1}^t \sum_{i=1}^n [(x_{Hy})_{Gen}]_{[t][i]} \cdot OPEX_{HFC}
\end{aligned}$$

Eq. 40

$$OPEX_{Non-Ren} = \sum_{t=1}^t \sum_{i=1}^n (x_{Nu})_{[t][i]} \cdot OPEX_{Nu}$$

Eq. 41

Objective function

The objective function of the optimization method is to minimize the total cost of energy production and absorption, taking into account the capital expenditures (CAPEX) and operational and maintenance expenses (OPEX) associated with each technology. This objective function is based on the concept of the levelized cost of energy (LCOE), which calculates the average cost of generating one unit of electricity over the project lifetime.

By evaluating the LCOE, the optimization method aims to find the scenario that results in the lowest overall cost per unit of energy produced and absorbed. This includes considering the costs of constructing and installing the energy generation infrastructure (CAPEX) as well as the ongoing operational and maintenance costs (OPEX) associated with each technology.

The objective function will assess and compare different alternatives, taking into account the LCOE values for each technology, to identify the scenario that offers the

most cost-effective and efficient solution for energy production and absorption in the system. By minimizing the total cost of energy, the objective function helps in determining the optimal mix and utilization of different resources to meet the energy demand while minimizing costs.

$$\min_{x \in \mathbb{R}} f(x) = LCOE_{Ren} + LCOE_{Non-Ren} \quad \text{Eq. 42}$$

5.2.2 General considerations

The assumptions outlined for the modelling of the Distributed Virtual Power Plant (DVPP) help to simplify and create a manageable model that represents the overall behaviour of the system. While these assumptions may not capture all the complexities and nuances of real-world scenarios, they provide a basis for initial analysis and optimization.

Energy dispatchability is instantaneous, and response times are negligible, assuming that producers can adjust their output quickly to match the demand. The power plant size for renewable sources is unlimited, meaning they can generate as much power as needed based on local environmental conditions. Nuclear power plant capacity remains constant, without increasing over time.

Producers within the DVPP are perfectly coordinated, allowing for optimal energy dispatch based on their individual LCOE values. The distance between distributed producers does not impact the performance of the grid, and grid losses are considered negligible.

Energy prices are not explicitly considered in the model. Instead, the levelized cost of energy (LCOE) is used as the metric for evaluating the cost-effectiveness of the DVPP. This approach simplifies the analysis by focusing on the cost of energy generation rather than market fluctuations.

System demand is based on base data from a national database for the year 2022. This data serves as a reference point for evaluating the energy requirements of the DVPP.

To reduce computational complexity, certain operational constraints such as ramp rates and minimum on/off times for power plants are not considered. Instead,

the limitations of energy storage systems are taken into account. The efficiency variation of the power plants during operation is considered negligible, allowing them to operate at their nominal conditions when required.

Transient elements in the grid, such as harmonics, parasitic losses, and reactive power injections, are neglected in the model. This assumption simplifies the analysis by considering the grid to operate in steady-state conditions at all times.

These assumptions provide a starting point for modelling and optimizing the DVPP, and they can be refined and adjusted as more accurate data and real-world considerations become available.

5.3 Optimization problem

5.3.1 Case 1 (Base case, limitation in installed capacity)

In the first approach of the model, the base scenario is analysed, where the energy system consists of various producers with a relatively low proportion of renewable energy. This configuration includes the presence of nuclear and gas power plants, along with 55% of renewable energy sources such as solar and wind.

The objective of the model is to optimize the energy system by determining the best combination of energy generation from these sources, taking into account the limitations and goals of the system. It seeks to minimize the overall cost, considering both the levelized cost of energy (LCOE) and the specific costs associated with each technology, such as investment expenses (CAPEX) and operating expenses (OPEX).

In the previous results obtained for this simulation for both communities, the incorporation of wind power facilities plays a significant role in the energy mix. The installed capacity of wind power exceeds that of photovoltaic (solar) energy, representing % of the total installed capacity. This highlights the importance of harnessing wind energy due to its relatively high-capacity factor, which indicates the effective energy production from a renewable source compared to its maximum capacity.

The capacity factor of wind energy generally surpasses that of solar energy, implying that wind turbines can generate electricity more consistently and for a longer duration. This is because wind resources are available both during the day and at

night, unlike solar power generation, which depends on the availability of sunlight. The intermittent nature of solar energy, due to diurnal and seasonal variations, emphasizes the importance of having a relatively continuous but still variable supply of wind energy in the energy mix.

In summary, the model recognizes the importance of wind energy in terms of availability and capacity factor, making it a key contributor in the energy mix along with other conventional and renewable sources. Another detail to consider is the presence of nuclear energy in Valencia, which provides a constant base generation that Andalusia does not have.

The following figures show the energy balance between demand and generation for Andalusia and Valencia.

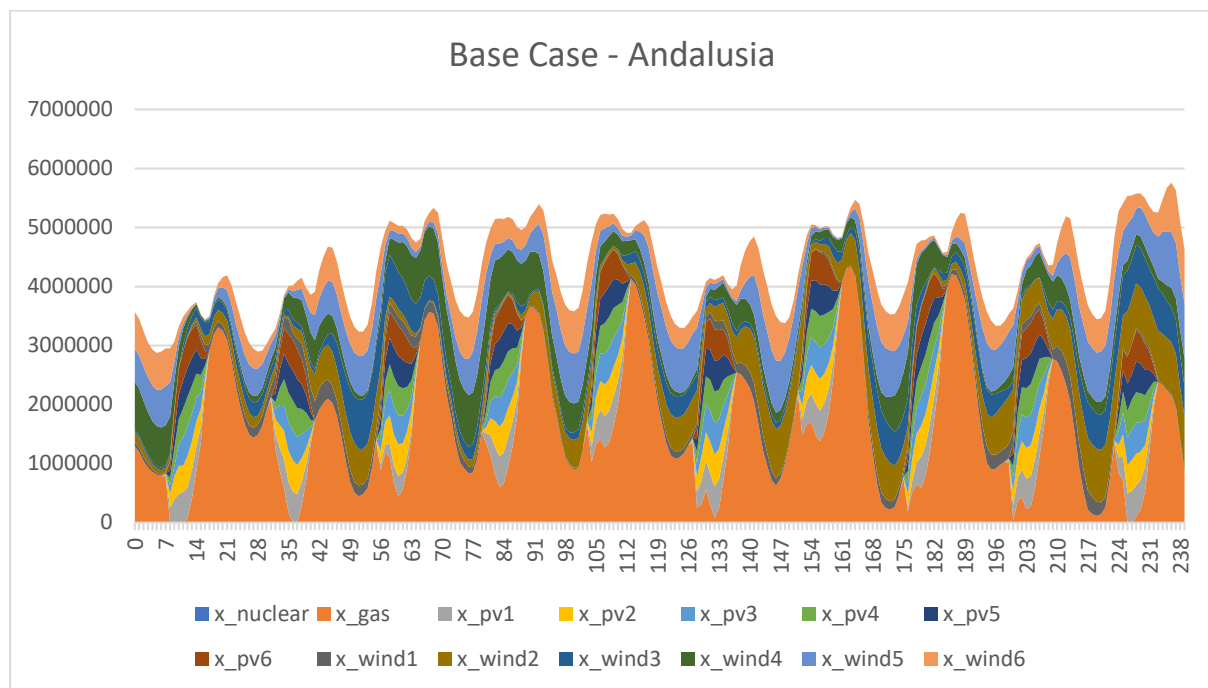


Illustration 35. Base case Matching Generation / demand in Andalusia

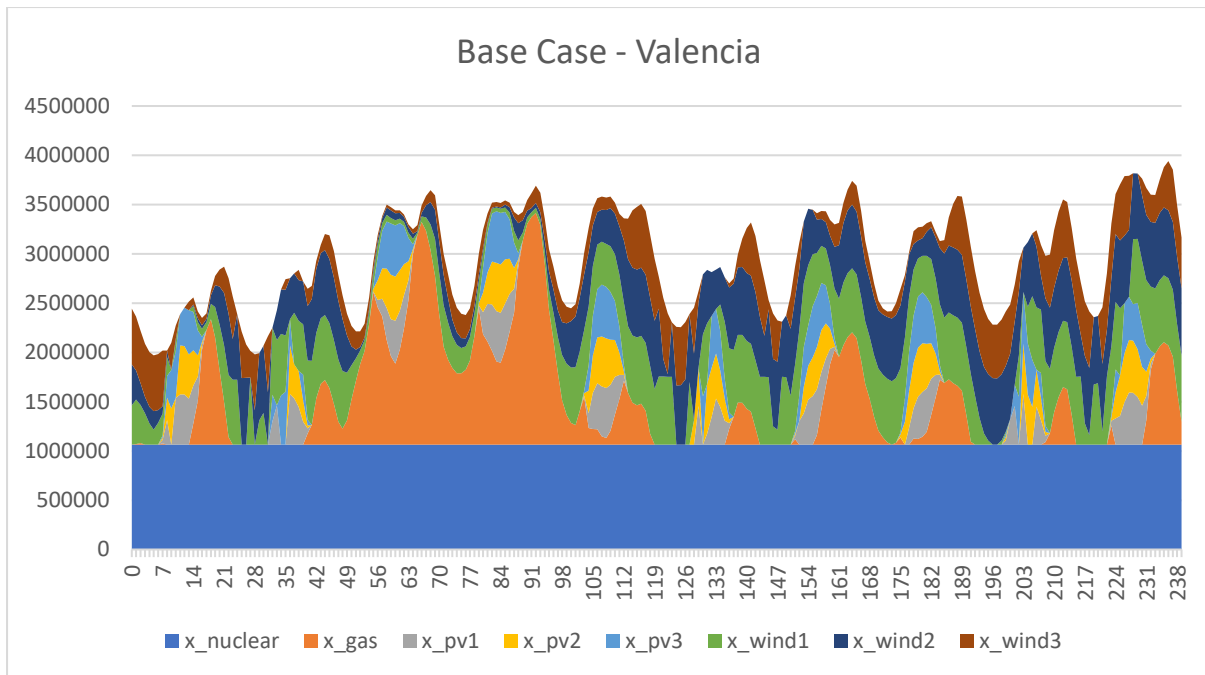


Illustration 36. Base case Matching Generation / demand in Valencia

5.3.2 Case 2 (increasing renewable share from 35 to 99%)

In the new scenario with a progressive increase in the renewable energy share, the model incorporates the same technologies as in the previous case (wind power and photovoltaics) but with a changing mix of installed capacity. The purpose is to analyse the behaviour of the total installed capacity and its impact on the Levelized Cost of Energy (LCOE).

As the renewable energy share increases, the model assumes that more wind power and photovoltaic facilities are added to the energy mix. This progressive increase in renewable capacity allows for a greater utilization of clean and sustainable energy sources while reducing reliance on conventional sources such as nuclear and gas.

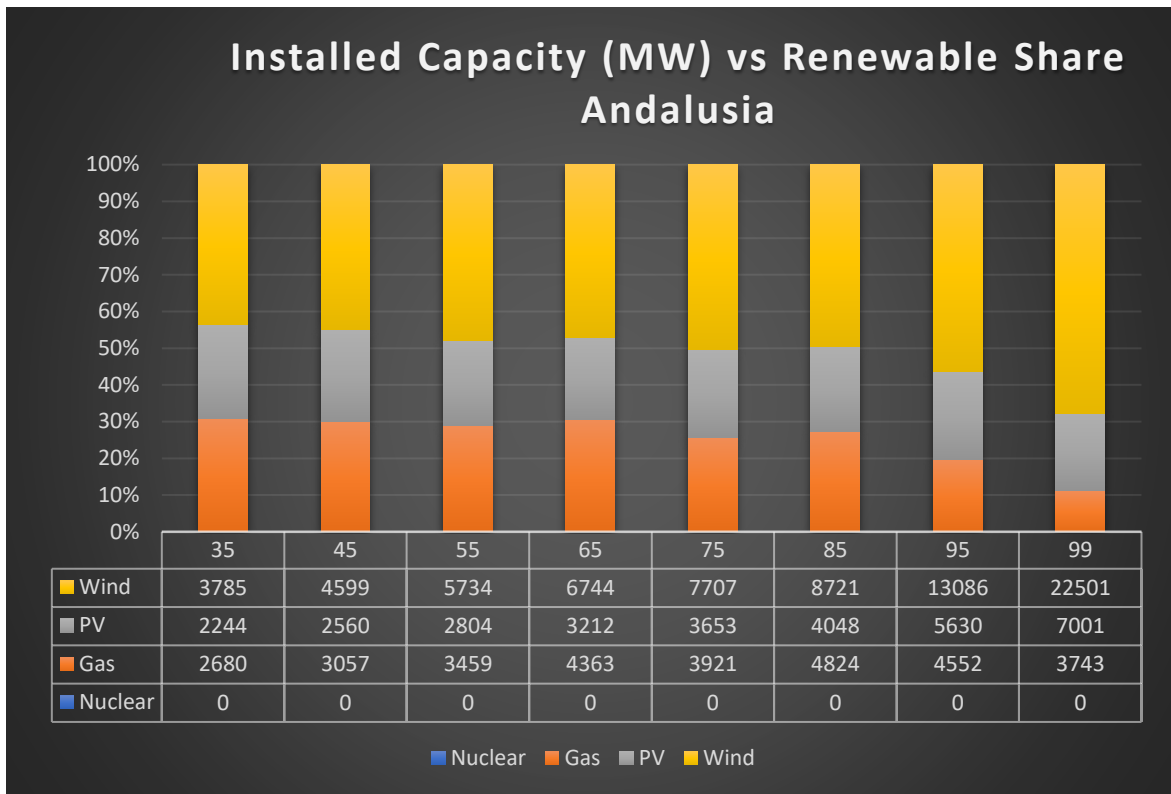


Illustration 37. Case 2 installed capacity vs Renewable share in Andalusia

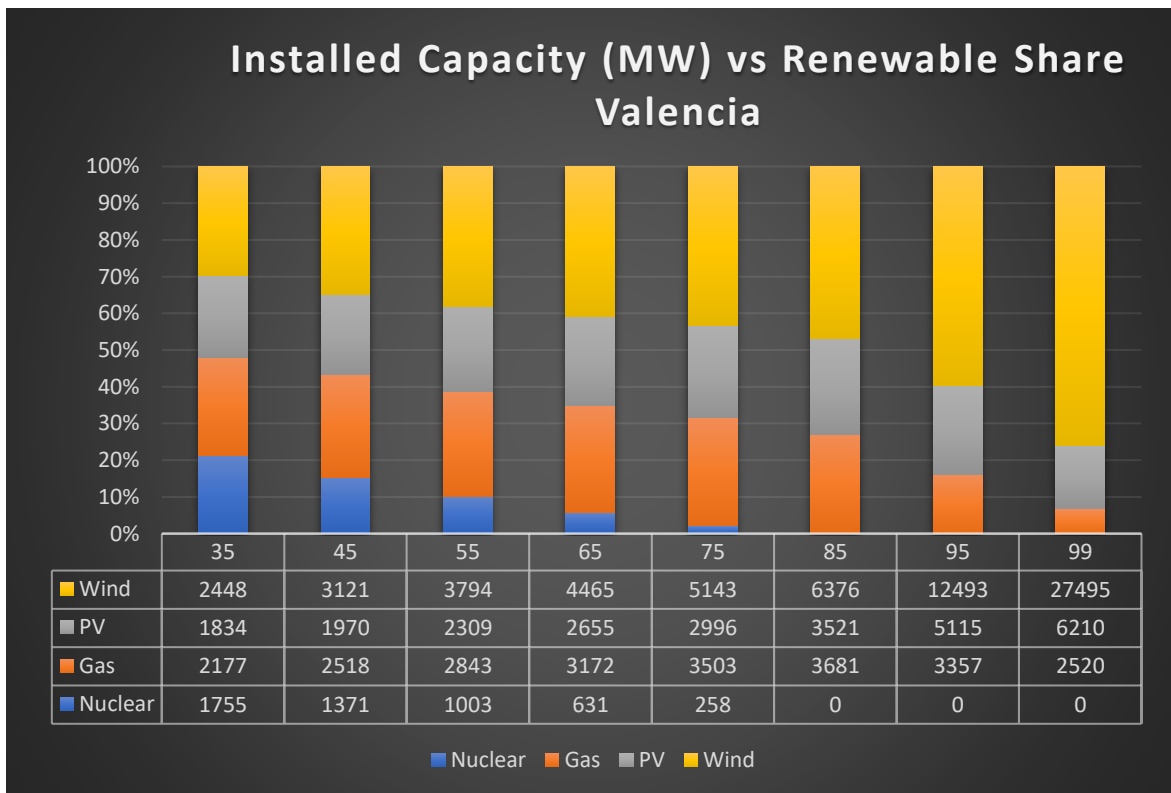


Illustration 38. Case 2 installed capacity vs Renewable share in Valencia

Illustration 37 and 38 provides a visual representation of the share of installed capacity specifically for wind energy. It shows that wind energy experiences a substantial increase in its share, starting from 44% at the initial 35% renewable share and reaching 67% at the 99% renewable share. This indicates the growing importance of wind power as the renewable share increases, highlighting its higher capacity factor compared to photovoltaics and its ability to provide a significant portion of the total installed capacity.

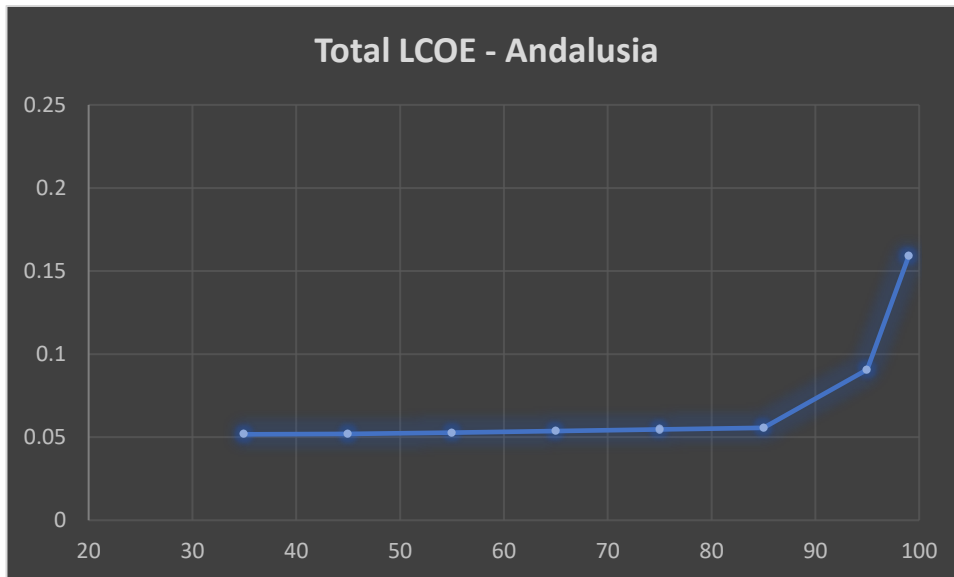


Illustration 39. Case 2 LCOE vs Renewable share in Andalusia

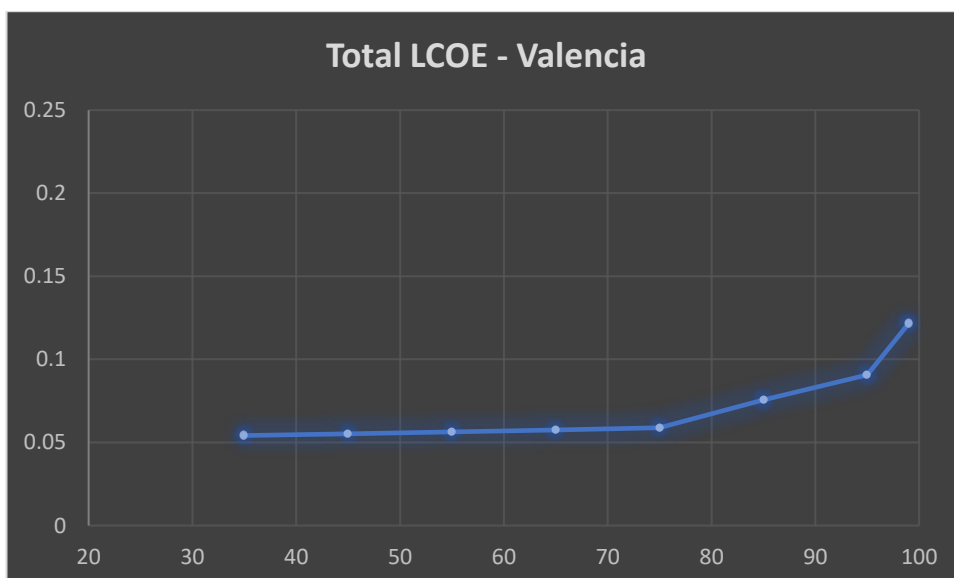


Illustration 40. Case 2 LCOE vs Renewable share in Valencia

Illustration 39 and 40 demonstrates the relationship between the levelized cost of energy (LCOE) and the renewable share. It shows that as the renewable share

increases, the LCOE of the system also increases. This indicates that the investment in renewable resources comes with a higher cost of implementation, particularly due to the unpredictable and variable nature of renewable sources like photovoltaics and wind power. To compensate for their intermittency, power plants need to be oversized, resulting in a lower capacity factor and higher overall costs compared to baseload generation sources such as nuclear and gas.

Overall, these findings suggest that the progressive increase in renewable share has implications for the capacity factors of different energy sources, with wind power playing a significant role. Additionally, the increase in renewable resources leads to higher LCOE, highlighting the challenges and costs associated with transitioning to a more renewable-based energy system. These insights can inform decision-making processes and help in evaluating the trade-offs between renewable integration and cost considerations.

5.3.3 Case 3 (increasing renewable share from 35 to 99% + Offshore)

In Case 3, offshore wind power is introduced as an additional energy source to the existing technologies in Case 2. The inclusion of offshore wind power adds another variable to consider, particularly due to its relatively high potential and associated costs.

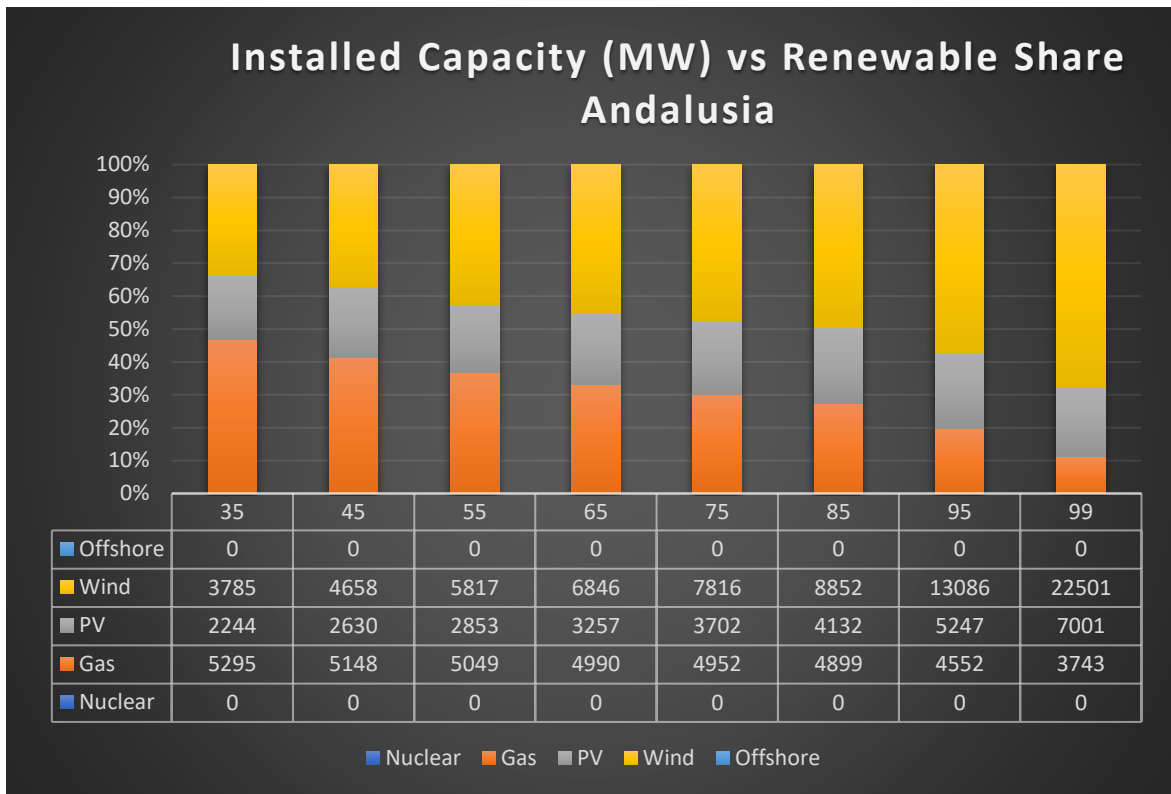


Illustration 41. Case 3 Installed Capacity vs Renewable share in Andalusia

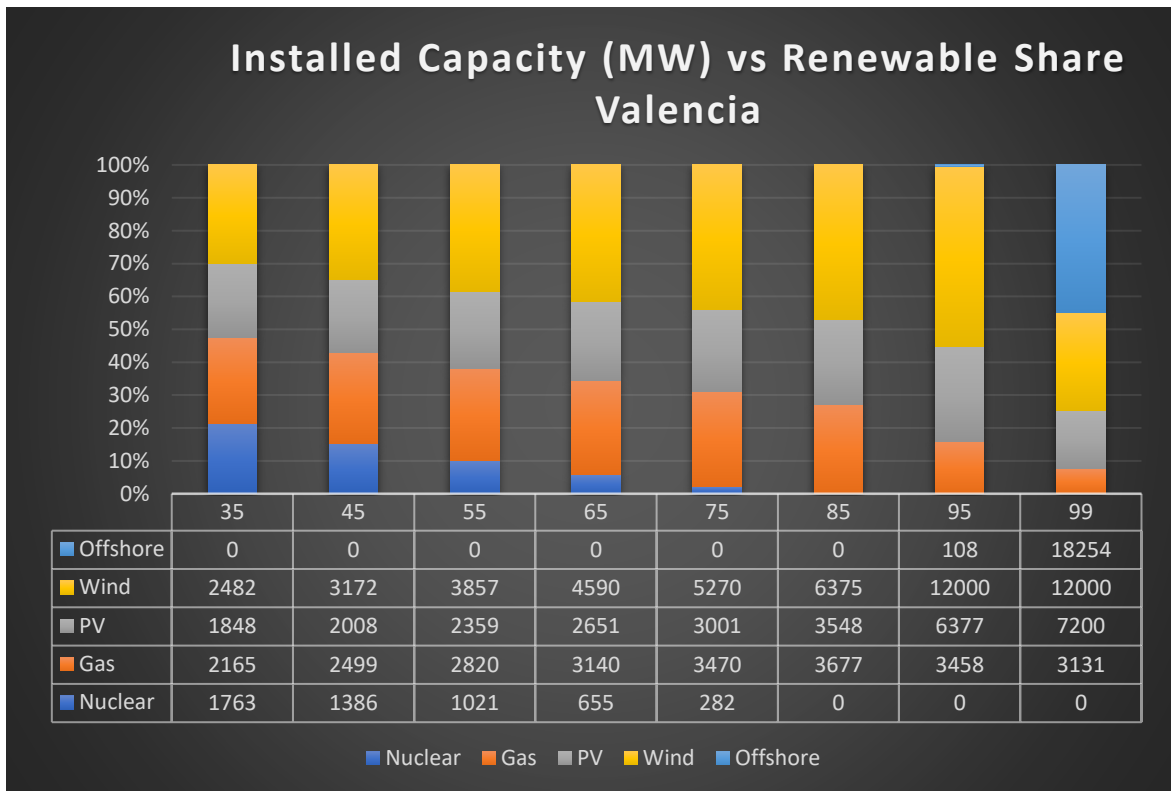


Illustration 42. Case 3 Installed Capacity vs Renewable share in Valencia

Illustration 41 and 42 demonstrates the dominant role of wind power in the installed capacity share, however, offshore wind power is not competitive enough to appear until 99% of renewable share (and due to power limitation of onshore facilities). As the renewable share increases, wind facilities (both onshore and offshore) benefit the most, while the contribution from photovoltaic remains relatively stable. This suggests that wind power, particularly offshore, becomes increasingly important in meeting the renewable energy targets.

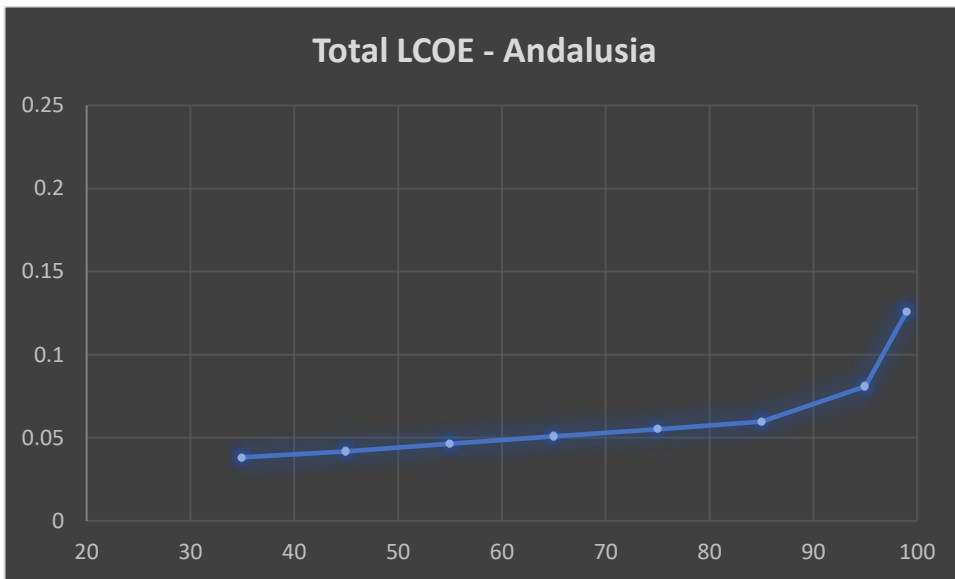


Illustration 43. Case 2 LCOE vs Renewable share in Andalusia

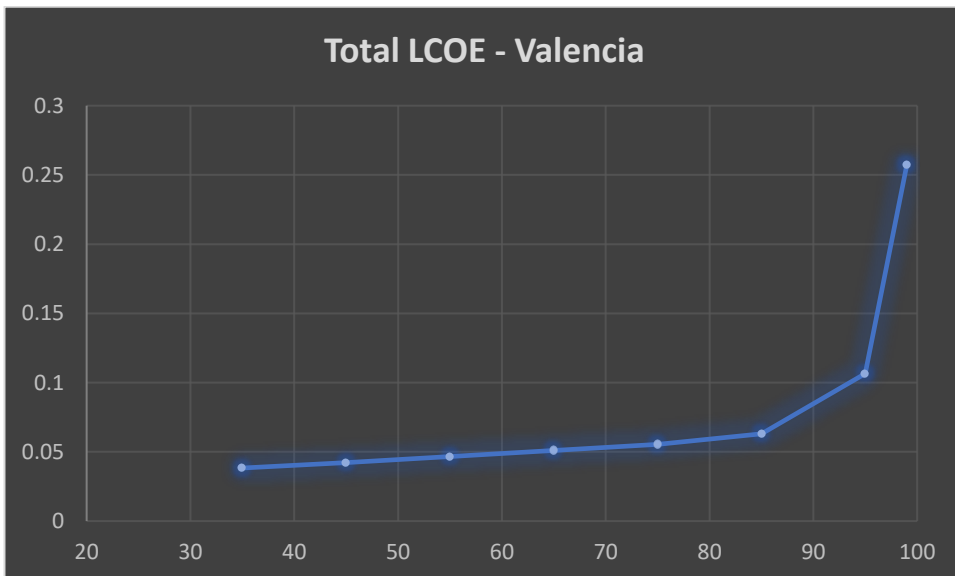


Illustration 44. Case 2 LCOE vs Renewable share in Valencia

Illustration 43 and 44 shows a gradual increase in the levelized cost of energy (LCOE) until the renewable share reaches 85%. At this point, when offshore wind power is incorporated into the model, the LCOE increases significantly. This indicates that the addition of offshore wind power, with its associated higher costs, has a considerable impact on the overall cost of the energy system.

The findings from Case 3 highlight the trade-offs between renewable integration, the role of offshore wind power, and the associated costs. The model incorporates offshore wind power only when necessary, indicating the need to optimize the energy mix based on the capabilities and cost-effectiveness of different technologies. It emphasizes the importance of carefully evaluating the potential and cost implications of incorporating offshore wind power into the energy system.

5.3.4 Case 4 (Renewable share from 35 to 99% + Offshore + Hydro + H2)

Case 4 builds upon Case 3, which explores the scenario by incorporating hydrogen and hydropower facilities and Hydrogen plants (with storage) as renewable sources to provide a stable basis. The behaviour of hydrogen and hydropower facilities is modelled similar to a battery, as discussed in section 5.2.1.

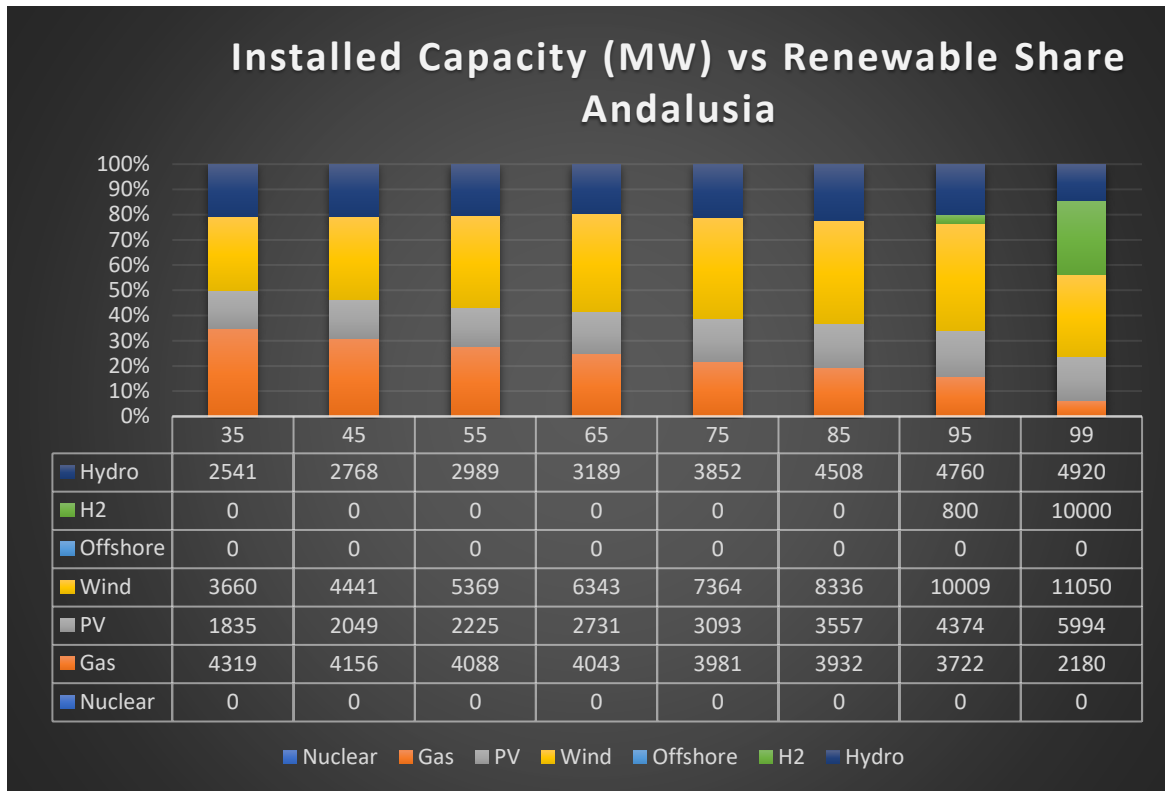


Illustration 45. Case 4 Installed Capacity vs Renewable share in Andalusia

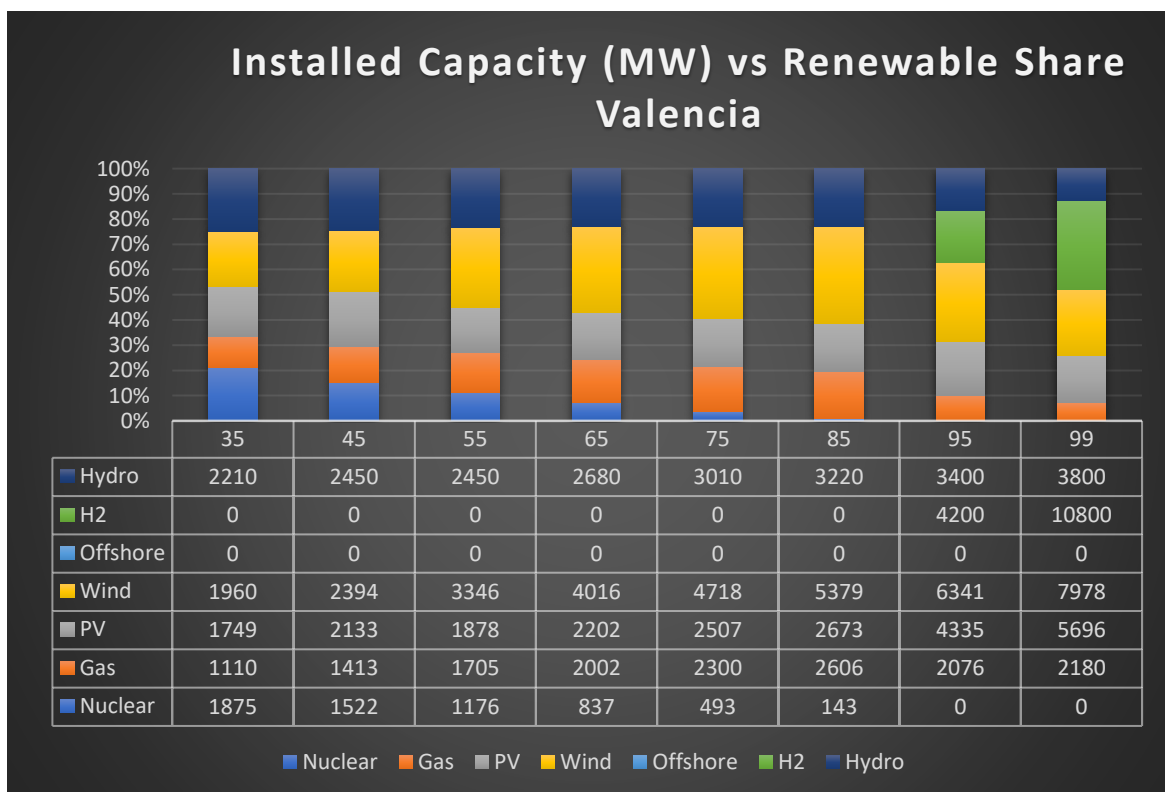


Illustration 46. Case 4 Installed Capacity vs Renewable share in Valencia

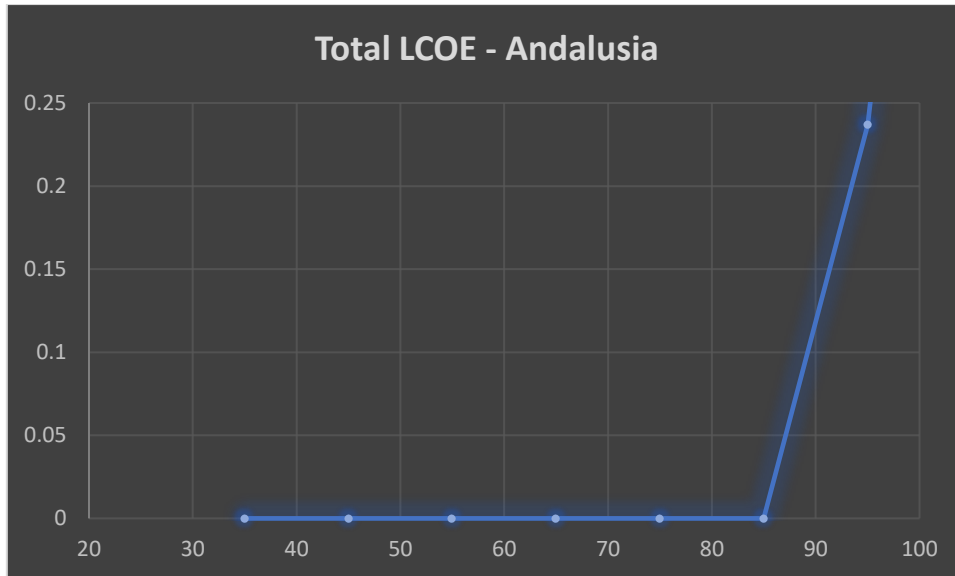


Illustration 47. Case 4 LCOE vs Renewable share in Andalusia

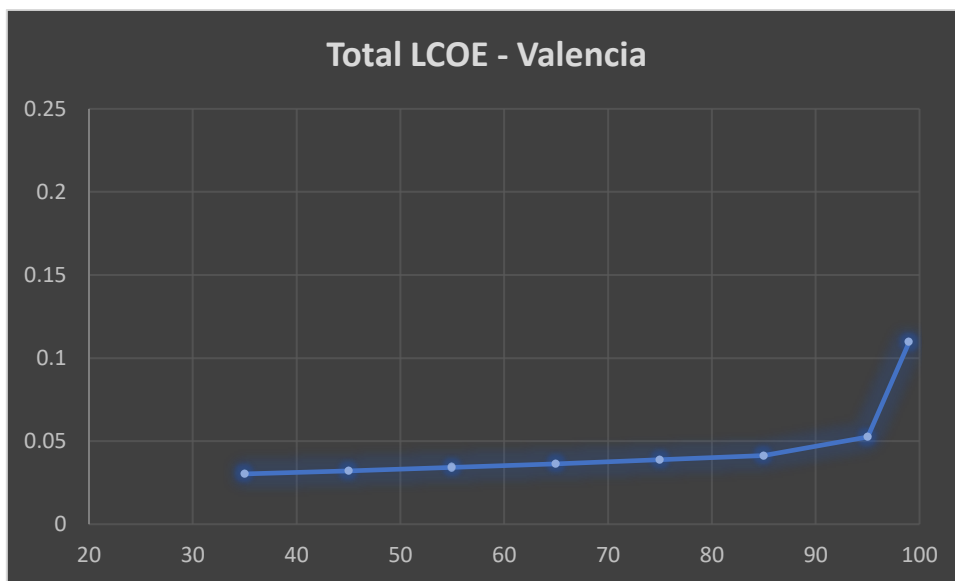


Illustration 48. Case 4 LCOE vs Renewable share in Valencia

The increase in the levelized cost of energy (LCOE) in Case 5 exhibits a gradual and exponential behaviour. At lower renewable shares, the increase in LCOE is relatively smaller compared to higher shares. This suggests that the addition of renewable storage systems, such as hydrogen and hydropower, not only contributes to electricity production but also enables energy storage and management. Incorporating storage systems can help mitigate the impact of intermittent renewable sources and contribute to a more stable and balanced energy system.

The findings from Case 5 highlight the potential benefits of incorporating storage technologies, such as hydrogen and hydropower, to enhance the stability and reliability of the renewable energy system. By enabling energy storage and management, these technologies can help address the variability of renewable sources and contribute to a smoother integration of renewable energy into the grid. Nevertheless, due to its high integration prices, they are not competitive enough to appear at low shares.

6 Conclusions and future improvements

The sizing of a power generation system has been addressed in different scenarios for two regions with distinct characteristics, such as Andalusia and Valencia. First, an optimization methodology has been developed, considering different sources (nuclear, gas, photovoltaic, onshore and offshore wind) as well as storage (hydrogen production and storage, pumped hydro), while minimizing costs. Then, the methodology was applied to various scenarios, and the results were analysed to understand the effect of each technology on the entire system.

It has been verified that costs escalate at high percentages of renewable penetration in all case studies. This is due to oversizing renewables in order to meet the entire demand. Furthermore, it has been demonstrated that incorporating storage helps reduce investment at higher levels of renewable penetration and reduces wasted energy resulting from curtailment. In this regard, hydro storage has been found to be the most efficient, but geographical limitations must be taken into account.

Regarding hydrogen systems, they appear when a high penetration of renewables is applied. However, this indicates that the system is not currently competitive due to prices, and therefore, it is not a solution with a significant impact on the modelling of power generation. Even with high renewable penetration, more than 50 plants with a production capacity of 60 MW and 200 MWh of storage would be required.

Additionally, it has been confirmed that offshore wind power plants are not competitive, but when geographical limitations are applied to onshore wind power plants, they become a viable alternative. The results also highlight the challenge of reducing gas infrastructure since, even though gas-based electricity production is a small part of the energy mix, infrastructure is needed for specific moments of the year

when renewables are insufficient. This leads to increased costs for higher percentages of renewables due to the fixed costs of gas. On the other hand, it has been found that even without renewable requirements, the most cost-effective solution already includes almost a 30% share of renewables.

In conclusion, the optimal solution lies in a delicate balance between renewable sources, storage, and conventional sources, aiming for the lowest possible cost. An important parameter in this balance is the desired percentage of renewables. The most accurate solution has been found to consider the majority of sources and constraints, resulting in an increasingly complex system formulation.

Future work in this field may include considering other sources such as solar thermal, incorporating ramp limitations, implementing a more realistic network model considering imports and exports, improving cost modelling, and considering demand management.

In general, it is recommended to aim for a 70-80% share of renewable energy. Based on economic results, costs start increasing exponentially at an 80% renewable share, but until then, they remain reasonable while achieving a significantly high amount of renewables. Considering resource availability and space, this target appears quite feasible, although the current renewable share in Spain is approximately 50%.

7 References

- [1] J. W. Tester, E. M. Drake, M. J. Driscoll, M. W. Golay and W. A. Peters, Sustainable Energy: Choosing Among Options, Cambridge: MIT Press, 2005.
- [2] International Energy Agency (IEA), "World Energy Outlook," November 2022. [Online]. Available: <https://iea.blob.core.windows.net/assets/830fe099-5530-48f2-a7c1-11f35d510983/WorldEnergyOutlook2022.pdf>. [Accessed 30 March 2023].
- [3] N. Srivastava, M. Srivastava, P. K. Mishra and V. K. Gupta, Microbial Strategies for Techno-economic Biofuel Production, Singapore: Springer Nature, 2020, pp. 173 - 198.
- [4] S. Gent, M. Twedt, C. Gerometta and E. AlMBERG, Theoretical and Applied Aspects of Biomass Torrefaction for Biofuels and Value-Added Products, vol. 23, Cambridge: Elsevier, 2017, p. 309.
- [5] S. Yusup and N. A. Rashidi, Value-chain of Biofuels: Fundamentals, Technology, and Standardization, Amsterdam: Elsevier, 2022, pp. 253 - 276.
- [6] S. Earle, Physical Geology, Victoria: BCcampus, 2019.
- [7] I. Dincer, Comprehensive Energy Systems, Amsterdam: Elsevier, 2021.
- [8] National Renewable Energy Laboratory (NREL), "Best Research-Cell Efficiency Chart," NREL, 21 March 2023. [Online]. Available: <https://www.nrel.gov/pv/cell-efficiency.html>. [Accessed 29 April 2023].
- [9] T. Soga, Nanostructured Materials for Solar Energy Conversion, vol. 4, Amsterdam: Elsevier, 2006, pp. 763 - 771.
- [10] G. N. Tiwari, A. Tiwari and S. , Handbook of Solar Energy: Theory, Analysis and Applications, vol. 21, Pensacola: Springer, 2016, pp. 1653 - 1658.

- [11] M. S. Răboacă, G. Badea, A. Enache, C. Filote, G. Răsoi, M. Rata, A. Lavric and R.-A. Felseghi, "Concentrating Solar Power Technologies," *Energies*, vol. 12, no. 6, p. 1048, 2019.
- [12] K. Johnson, G. Dalton and I. Masters, *Building Industries at Sea: 'Blue Growth' and the New Maritime Economy*, Gistrup : River Publishers, 2018.
- [13] Wikipedia, "Rance Tidal Power Station," Wikipedia, 07 May 2023. [Online]. Available: <https://tethys.pnnl.gov/project-sites/la-rance-tidal-barrage>. [Accessed 15 May 2023].
- [14] M. Basu and S. Xavier, *Fundamentals of Environmental Studies*, Delhi: Cambridge University Press, 2016.
- [15] N. Vukajlovic, V. Katic, D. Milicevic, B. Dumnic and B. Popadic, "Active Control of Induction Generator in Ocean Wave Energy Conversion System," in *Smart Electricity Distribution Grids Based on Distribution Management System and Distributed Generation*, Novi Sad, 2018.
- [16] IEA-RETD, *Offshore Renewable Energy: Accelerating the Deployment of offshore wind, tidal and wave technologies*, vol. 1, New York: Earthscan, 2012, pp. 262 - 276.
- [17] M. I. Cusano, Q. Li, A. Obisesan, J. Urrego-Blanco and T. H. Wong, *Coastal City and Ocean Renewable Energy: Pathway to an Eco San Andres*, vol. 8, Southampton: University of Southampton, 2013.
- [18] W. Tiju, T. Marnoto, S. Mat, M. Ruslan and K. Sopian, "Darrieus vertical axis wind turbine for power generation I: Assessment of Darrieus VAWT configurations," *Renewable Energy*, vol. 75, pp. 50 - 67, 2015.
- [19] Z. Tasneem, A. A. Noman, S. K. Das, D. K. Saha, R. Islam, F. Ali, F. R. Badal, H. Ahamed, S. I. Moyeen and F. Alam, "An analytical review on the evaluation of wind resource and wind turbine for urban application: Prospect and challenges," *Developments in the Built Environment*, vol. 4, p. 15, 2020.

- [20] M. De Lellis, R. Reginatto, R. Saraiva and A. Trofino, "The Betz limit applied to Airborne Wind Energy," *Renewable Energy*, vol. 127, pp. 32 - 40, 2018.
- [21] Wind Turbine Models, "Gamesa G80 - 2,00 MW - Wind Turbine," Lucas Bauer & Silvio Matysik, [Online]. Available: <https://en.wind-turbine-models.com/turbines/34-gamesa-g80>. [Accessed 18 April 2023].
- [22] S. Sivanagaraju, M. Reddy and D. Srilatha, *Generation and Utilization of Electrical Energy*, New Delhi: Pearson, 2010.
- [23] A. J. Omosanya, E. T. Akinlabi and O. Okeniyi, "Overview for Improving Steam Turbine Power Generation Efficiency," in *Journal of Physics: Conference Series*, 2019.
- [24] S. Bhatia, *Advanced Renewable Energy Systems*, Boca Raton: CRC Press, 2014.
- [25] E. Hossain, *The Sun, Energy, and Climate Change*, Cham: Springer Nature, 2023.
- [26] T. A. Parish, V. V. Khromov and I. Carron, *Safety Issues Associated with Plutonium Involvement in the Nuclear Fuel Cycle*, Heidelberg: Springer, 2012.
- [27] A. Basile and A. Iulianelli, *Advances in Hydrogen Production, Storage and Distribution*, Cambridge: Elsevier, 2014.
- [28] E. Iglesia, J. Spivey and T. Fleisch, *Natural Gas Conversion VI*, Amsterdam: Elsevier, 2001.
- [29] C. A. Grimes, O. K. Varghese and S. Ranjan, *Light, Water, Hydrogen: The Solar Generation of Hydrogen by Water Photoelectrolysis*, New York: Springer, 2008.
- [30] B. Grewal, N. Hendriyetty, I. Abdullaev, C. J. Kim, N. Yoshino and E. K. Ayoob Ayoobi, *Unlocking Private Invest in Sustainable Infrastructure in Asia*, New York: Routledge, 2023.
- [31] M. Hirscher, *Handbook of Hydrogen Storage: New Materials for Future Energy Storage*, Weinheim: Wiley-VCH, 2010.

- [32] C. O. Colpan and A. Kovač, Fuel Cell and Hydrogen Technologies in Aviation, Cham: Springer, 2022.
- [33] World Intellectual Property Organization, Patent Landscape Report - Hydrogen fuel cells in transportation, Geneva: WIPO, 2022.
- [34] K. E. Cox and K. D. Williamson, Hydrogen: Its Technology and Implications, Boca Raton: CRC Press, 1997.
- [35] L. O. Williams, Hydrogen Power: An Introduction to Hydrogen Energy and its Applications, New York: Pergamon Press, 1980.
- [36] F. Sen, A. Khan and A. M. Asiri, Nanomaterials for Hydrogen Storage Applications, Amsterdam: Elsevier, 2021.
- [37] J. H. Kelley and E. A. Laumann, Hydrogen Tomorrow: Demands & Technology Requirements, California, 1975.
- [38] L. M. Gandía, G. Arzamendi and P. M. Diéguez, Renewable Hydrogen Technologies: Production, Purification, Storage, Application and Safety, Amsterdam: Elsevier, 2013.
- [39] M. Jaunatre, Renewable Hydrogen: Renewable Energy and Renewable Hydrogen APAC Markets Policies Analysis, Wiesbaden: Springer, 2021.
- [40] A. Orsini and E. Kavvatha, EU Environmental Governance: Current and Future Challenges, London: Taylor & Francis, 2020.
- [41] E. Woerdman, M. Roggenkamp and M. Holwerda, Essential EU Climate Law, Cheltenham: Edward Elgar Publishing Limited, 2021.
- [42] I. J. Visseren-Hamakers and T. J. Kok, Transforming Biodiversity Governance, Cambridge: Cambridge University Press, 2022.
- [43] European Commission, "Circular economy action plan," European Commission, [Online]. Available: https://environment.ec.europa.eu/strategy/circular-economy-action-plan_en. [Accessed 20 May 2023].

- [44] A. Negm, L. Zaharia and G. Ioana-Toroimac, *The Lower Danube River: Hydro-Environmental Issues and Sustainability*, Cham: Springer, 2022.
- [45] A. Zangeneh and M. Moeini-Aghtaie, *Scheduling and Operation of Virtual Power Plants: Technical Challenges and Electricity Markets*, Cambridge: Elsevier, 2022.
- [46] H. Schulte and S. Kusche, "Demanded Power Point Tracking of PV Power Plants without Battery Energy Storage," in *Proceedings 31. Workshop Computational Intelligence*, Karlsruhe, KPS Scientific Publishing, 2021, pp. 169 - 188.
- [47] A. Sallam and O. Malik, *Electric Distribution Systems*, Hoboken: Wiley, 2019.
- [48] D. Tungadio and Y. Sun, "Load frequency controllers considering renewable energy integration in power system," *Energy Reports*, vol. 5, pp. 436 - 453, 2019.
- [49] L. Meegahapola, S. Bu and M. Gu, *Hybrid AC/DC Power Grids: Stability and Control Aspects*, Cham: Springer, 2022.
- [50] R. Belu, *Smart Grids Fundamentals: Energy Generation, Transmission and Distribution*, Boca Raton: CRC Press, 2022.
- [51] A. Chakrabarti and S. Halder, *Power System Analysis: Operation and Control*, Delhi: PHI Learning Private Limited, 2022.
- [52] S. Das, R. Islam and W. Xu, *Advances in Control Techniques for Smart Grid Applications*, Singapore: Springer, 2022.
- [53] O. Edenhofer, r. Pichs Madruga and Y. Sokona, *Renewable Energy Sources and Climate Change Mitigation: Special Report of the Intergovernmental Panel on Climate Change*, Cambridge: Cambridge University Press, 2012.